Humidity Control for Indoor Farms

Final Report

ET24SWE0064

Prepared by:

Graham Jaeger UC Davis Western Cooling Efficiency Center

Theresa Pistochini UC Davis Western Cooling Efficiency Center

July 30, 2026

Program paid for by ratepayers.

Disclaimer

The CalNEXT program is designed and implemented by Cohen Ventures, Inc., DBA Energy Solutions ("Energy Solutions"). Southern California Edison Company, on behalf of itself, Pacific Gas and Electric Company, and San Diego Gas & Electric® Company (collectively, the "CA Electric IOUs"), has contracted with Energy Solutions for CalNEXT. CalNEXT is available in each of the CA Electric IOU's service territories. Customers who participate in CalNEXT are under individual agreements between the customer and Energy Solutions or Energy Solutions' subcontractors (Terms of Use). The CA Electric IOUs are not parties to, nor guarantors of, any Terms of Use with Energy Solutions. The CA Electric IOUs have no contractual obligation, directly or indirectly, to the customer. The CA Electric IOUs are not liable for any actions or inactions of Energy Solutions, or any distributor, vendor, installer, or manufacturer of product(s) offered through CalNEXT. The CA Electric IOUs do not recommend, endorse, qualify, guarantee, or make any representations or warranties (express or implied) regarding the findings, services, work, quality, financial stability, or performance of Energy Solutions or any of Energy Solutions' distributors, contractors, subcontractors, installers of products, or any product brand listed on Energy Solutions' website or provided, directly or indirectly, by Energy Solutions. If applicable, prior to entering into any Terms of Use, customers should thoroughly review the terms and conditions of such Terms of Use so they are fully informed of their rights and obligations under the Terms of Use, and should perform their own research and due diligence, and obtain multiple bids or quotes when seeking a contractor to perform work of any type.

Executive Summary

This report presents findings from a field demonstration of an all-electric heating, ventilation, and air conditioning (HVAC) system designed to meet the unique dehumidification demands of indoor farming. The project compares this system, which consists of a conventional air conditioning system paired with a heat recovery heat exchanger, to a conventional air conditioning system with electric resistance reheat in two container farms that grow lettuce. The demonstration evaluated energy and demand savings, operational performance under real-world growing conditions, and comparison to prior lab-based performance data and modeling.

Both farms (Farm 1 and Farm 2) were initially equipped with the same HVAC system and were instrumented in December 2024 with a sensing and data acquisition system. In July 2025, Farm 1 was retrofitted with the energy-efficient HVAC system, which this report describes in detail. Monitoring continued after the retrofit, through May 2026. Although the task order only required side-by-side post-retrofit evaluation, both pre-retrofit and post-retrofit results are presented. Post-retrofit results are further split into three distinct analysis periods, each marked by improvements made to the retrofit HVAC system.

In the pre-retrofit monitoring period (December 14, 2024, to May 31, 2025), the indoor relative humidity for both farms frequently exceeded target levels, particularly when the artificial grow lights were off. In the first post-retrofit monitoring period, which ran from August 14 to November 11, 2025, the retrofit system easily satisfied the relative humidity setpoint in Farm 1 but occasionally struggled to meet the farm's temperature setpoint. This indicated that the equipment provided too much dehumidification but not enough sensible cooling. Farm 2 remained too humid in this period, which the research team determined at the end of the study was likely attributed to a bias in the relative humidity sensor controlling the baseline HVAC system.

In mid-November 2026, the research team installed a custom air bypass duct that increased the retrofit system's sensible cooling capacity. The installation of this custom bypass distinguishes the first post-retrofit period from the second, which ran from November 20, 2025, to January 5, 2026. In this period, the retrofit system consistently met the relative humidity and temperature setpoints in Farm 1, while Farm 2 remained too humid.

On January 6, 2026, the team updated the HVAC control algorithm at Farm 1 to enable further energy savings with the retrofit system. The last post-retrofit period encapsulates January 7 to May 7, 2026. In this period, the retrofit system consistently met the relative humidity setpoint but occasionally struggled to meet the temperature setpoint on hot days. While the bypass improved conditions at Farm 1, it did not completely resolve the issue in hot weather. Farm 2 remained too humid, as it did in other periods.

Across all periods of the study, the loads from the farms' artificial grow lights, which are the primary source of heat in the farm, were nearly identical for both farms. However, notable differences emerged in HVAC energy consumption. In the pre-retrofit period, the average HVAC energy use was 108 kilowatt-hours per day at Farm 1 and 91 kilowatt-hours per day at Farm 2. The difference was statistically significant and was likely caused by the sensor offset issue, as well as tree shade at Farm 2 that reduced heat transfer from the environment to the farm. In the three post-retrofit periods, the retrofit HVAC system at Farm 1 used significantly less energy per day than the baseline

HVAC system at Farm 2. We observed average energy savings of 37.1 percent, 41.1 percent, and 40.9 percent in the first, second, and third post-retrofit periods, respectively. These savings were attributed to reduced reheat energy. Similarly, Farm 1 experienced reductions in on-peak energy use of 29.5 percent, 29.8 percent, and 24.8 percent in the post-retrofit periods.

Given that the sensor offset issue and tree shade at Farm 2 likely led to more humid indoor conditions and lower HVAC energy use at Farm 2 across the study, we also compared Farm 1's pre-retrofit period—when Farm 1 operated with the baseline HVAC system—to Farm 1's third post-retrofit period—when Farm 1 operated with the finalized retrofit system. These two periods spanned the same months with comparable weather in 2025 and 2026, respectively, enabling a valid comparison. We observed energy savings of 59.3 percent with the retrofit system relative to the baseline. We also developed curves to predict daily HVAC energy use of both the baseline retrofit systems based on daily average outdoor air temperature. Using typical meteorological year weather data for the location of the demonstration site, we forecasted that the retrofit system is expected to provide 51.5 percent annual energy savings relative to the baseline system at Farm 1 under typical weather.

The team further explored the cooling performance of the retrofit system and the baseline HVAC in detail for the third post-retrofit period, when the retrofit system operated at its peak. We analyzed the retrofit system's sensible cooling capacity, latent cooling capacity, and Coefficient of Performance relative to the baseline HVAC at Farm 2 in the same period and to previous laboratory testing results. We found that the retrofit system was generally more impacted by increasing outdoor air temperature than the baseline HVAC and that the performance metrics obtained from laboratory testing were generally higher than the results obtained from field testing. Field data from this period were also used to develop equipment performance models for both the retrofit system and the baseline HVAC, which will enable future efforts to model indoor container farms.

Stakeholder engagement primarily involved sharing results with and collecting feedback from the operators of the indoor farm, the manufacturers and distributors of the retrofit system, and the manufacturers of the indoor farms themselves. Farm operators mainly offered feedback related to the challenges of the retrofit process and the initial equipment startup. The retrofit took about three weeks, during which the farm was offline—a difficult situation for a facility that operates year-round. However, most of these challenges reflect the difficulty of scheduling retrofits and construction rather than issues with the technology itself. The manufacturer of the retrofit system, the distributor of the equipment, and the container farm manufacturer all expressed a strong interest in the project at the beginning of the study and supported it intermittently throughout. Lastly, the team presented preliminary findings at the 2026 ASHRAE Winter Conference and will publish the final results at the conclusion of the study.

As discussed above, this study shows that the retrofit system can provide substantial energy savings at a real-world indoor farm. However, it is not without challenges—for example, the compressor failed twice during the study. The first failure occurred in November 2025; this was explained by a lack of appropriate low-ambient controls, which we corrected. The second failure occurred in July 2026 and is currently under investigation. One possibility is that frequent compressor cycling during the winter—which can reach 150 cycles per day—caused the failure. This frequent cycling could easily be reduced by an increase in the deadband for the humidity control of the farm, but it is unclear at this

time if that would resolve the problem. We have engaged the equipment distributor for further investigation and implementation of a solution.

Additionally, the system occasionally did not have enough sensible cooling capacity to meet temperature setpoints during peak loads and hot weather. Therefore, it is critical that indoor farms seeking to replace their HVAC systems with the retrofit system incorporate a means to increase the sensible cooling capacity when needed. The team accomplished this with a low-cost custom air bypass, but future research should be conducted to explore other methods, such as installing a secondary cooling coil. Furthermore, to enable widespread adoption in container farms, the geometry of technology would need to be redesigned to reduce installation costs.

Abbreviations and Acronyms

Acronym	Meaning
AHU	Air handling unit
CFM	Cubic feet per minute
COP	Coefficient of Performance
CO_2	Carbon dioxide
gpd/ ft^2	Gallons per day per square foot
HVAC	Heating, ventilation, and air conditioning
kBTU/h	Kilo-British thermal units per hour
kPa	Kilopascal
kW	Kilowatt
kWh	Kilowatt-hour
PH	Pre-reheat
PLC	Programmable logic controller
R^2	Coefficient of determination
RA	Return air
RH	Relative humidity
RSE	Residual standard error
SHR	Sensible heat ratio
T	Temperature
TMY	Typical meteorological year
TXV	Thermostatic expansion valve
V	Volt

Acronym	Meaning
VPD	Vapor pressure deficit
W/ft^2	Watts per square foot
WCEC	Western Cooling Efficiency Center

Contents

Executive Summary iii
Introduction 1
Background 1
Indoor Farming 1
HVAC Loads in Indoor Farms 1
State-of-the-Art Dehumidification Approaches 2
Previous Research 4
Objectives 4
Methodology and Approach 5
Test Site(s) 5
Test Plan 8
Findings 19
Overview 19
Results: All Monitoring Periods 21
Results: Period 4 with Refined Retrofit HVAC Operation 29
Results: Modeling Inputs 34
Data Analysis 40
Stakeholder Feedback 42
Recommendations 43
Limitations 43
Future Research 44
References 45
Appendix 46

Tables

Table 1: Instrumentation of baseline HVAC system. 9
Table 2: Sensors added during the retrofit. 12
Table 3: Operating modes for baseline HVAC. 17
Table 4: Operating modes for the retrofit system. 17
Table 5: Time periods, date ranges, and operating conditions. 20
Table 6: Lighting energy use at each farm across all periods. 21
Table 7: Analysis of VPD frequency for each farm across all analysis periods. 24
Table 8: Best fit equations and adjusted R^2 values. 28
Table 9: Best-fit equipment performance curve coefficients for the retrofit system in cool mode. 37
Table 10: Best-fit equipment performance curve coefficients for the retrofit system in dehumidify mode. 38
Table 11: Domain for input data for best-fit equipment curves for the retrofit system. 38
Table 12: Best-fit equipment performance curve coefficients for baseline HVAC in cool mode. 39
Table 13: Domain for input data for best-fit equipment curves for baseline HVAC. 40
Table 14: Comparison of predicted results derived from a model created from field data to laboratory test results. 40

Figures

Figure 1: Diagrams of HVAC approaches for indoor farming. 4
Figure 2: Container farm nursery area (left), cultivation walls, and lighting panels (right). 6
Figure 3: Grow light schedule observed in both farms during standard time (left) and daylight saving time

(right). 7
Figure 4: Side view of farm interior and baseline HVAC system. 8
Figure 5: Diagram showing sensor locations inside farm and baseline HVAC system. 9
Figure 6: Instrumentation installed to monitor the baseline HVAC systems at both farms. 10
Figure 7: The retrofit system system installed at Farm 1. 11
Figure 8: Sensor locations in the retrofit system. 12
Figure 9: Diagram of airflow through the retrofit system with the partial heat exchanger bypass installed. 14
Figure 10: Partial heat exchanger bypass return duct connection with damper (left) and AHU connection with filter box (right). 14
Figure 11: Original retrofit control system algorithm. 15
Figure 12: Improved retrofit control system algorithm. 16
Figure 13: Histograms of each farm's VPD distribution across all periods, disaggregated by lights on/off. 23
Figure 14: Bar graphs of average daily HVAC energy use for each farm across all analysis periods, disaggregated by HVAC component and lights on/off. 25
Figure 15: Bar graph depicting the average daily on-peak HVAC energy use at each farm in each period. 27
Figure 16: Farm 1's daily HVAC energy use versus average daily outdoor air temperature in Periods 1 and 4. 28
Figure 17: HVAC mode frequency versus outdoor air temperature for Farm 1 and Farm 2 during Period 4. 29
Figure 18: Plots of latent capacity and sensible capacity for three cooling and dehumidification modes in both farms. 31
Figure 19: Plots of total COP for three cooling and dehumidification modes in both farms. 32
Figure 20: Plots of field and laboratory sensible and latent capacity (left) and COP (right) for the retrofit system in dehumidify mode. 33
Figure 21: Plots of hourly external heat flux versus hourly average outdoor air temperature for Farm 1 (left) and Farm 2 (right). 35
Figure 22: Average daily moisture generation rates for Farm 1 (left) and Farm 2 (right) in Period 4. 36
Figure 23: Presentation at ASHRAE 2026 Winter Conference. 43
Figure 24: Modeled performance curves for the retrofit system, cool mode. 46
Figure 25: Modeled performance curves for the retrofit system, dehumidify mode. 47
Figure 26: Modeled performance curves for baseline HVAC, cool mode. 48

Introduction

This report presents findings from a field demonstration of an all-electric heating, ventilation, and air conditioning (HVAC) system designed to efficiently manage the high latent loads typical in indoor farming. The study compared the retrofit system, which consists of a conventional air conditioning system paired with a heat recovery heat exchanger, to a conventional air conditioning system with electric resistance reheat, using two side-by-side container farms that grow lettuce. The retrofit system uses a plate heat exchanger and variable-speed fan to dehumidify while minimizing overcooling and the need for reheat.

The goals of the demonstration were to evaluate energy and demand savings, assess real-world performance in managing cooling and dehumidification loads, and compare field data to prior laboratory testing and modeling. The report also documents installation and operational experience to inform broader market adoption.

The findings presented in this report are final and include performance data from both container farms before and after the team replaced one farm's HVAC equipment with the retrofit system. Additionally, the report includes background on HVAC loads in indoor farms, describes the demonstration site and equipment, documents the retrofit process, discusses challenges faced by the retrofit equipment and solutions taken to resolve them, presents results and observations, develops equipment performance curves to enable modeling of indoor container farms, and summarizes stakeholder engagement supporting tech transfer.

Background

Indoor Farming

Indoor farming is a type of controlled environment agriculture, which describes farming operations that seek to regulate growing conditions to boost crop growth. Indoor farms have insulated, opaque building envelopes and use artificial lighting to grow crops; in these farms, irrigation, temperature, and humidity are tightly controlled, and crops are typically grown in dense vertical columns. Indoor farms are attractive, as they can provide hyperlocal produce in a small footprint, reduce pest and pathogen exposure, and save water relative to outdoor farming (UC Davis College of Agricultural and Environmental Sciences 2025). However, maintaining the indoor environment at optimal growing conditions is energy-intensive, which is a major barrier to further adoption. Artificial lighting and HVAC are the two largest energy end-uses in indoor farms, with HVAC often accounting for 45 percent of total energy use (Stober and Weitze 2024). Therefore, improving HVAC energy efficiency is an important opportunity to increase the viability of indoor farming.

HVAC Loads in Indoor Farms

In air conditioning systems, total cooling consists of sensible and latent components: sensible cooling is the reduction of the air's dry-bulb temperature, and latent cooling is the removal of moisture from the air through dehumidification. In most commercial and residential buildings in the

western United States, HVAC systems are designed to deliver primarily sensible cooling, typically accounting for 70 to 100 percent of the total cooling load.

In contrast, indoor farming environments have high latent loads, meaning dehumidification is the dominant cooling requirement. Moisture is added to the space through irrigation and plant transpiration, while the grow lights drive plant growth and contribute to sensible heat. The use of high-efficiency light-emitting diode lighting minimizes the sensible load. As a result, the objective becomes removing moisture from the air as efficiently as possible, while providing only a small amount of sensible cooling to maintain the desired space temperature.

The best practice for indoor farming HVAC is to control the indoor environment to maintain a desired vapor pressure deficit (VPD). VPD represents the "pressure" that air exerts to draw water from plants through transpiration—dry air (high VPD) pulls more moisture, while humid air (low VPD) reduces that pull. When VPD is too high and plants are not adequately watered, they may wilt or suffer from nutrient transport issues such as calcium deficiency, which appears as leaf-tip burn in lettuce. In contrast, because moisture lingers on leaf surfaces, a VPD that is too low can slow growth, reduce nutrient uptake, and create an environment more favorable for fungal and bacterial diseases. For lettuce, maintaining a VPD around 0.8 kilopascals (kPa) to 1.0 kPa strikes a healthy balance by promoting growth and efficient nutrient uptake while avoiding excessive stress (Sabeh 2020). Additionally, higher VPD increases demand on HVAC systems and irrigation—requiring more dehumidification capacity and water use—so controlling VPD at target levels helps optimize both plant performance and operational efficiency.

VPD is a function of the relative humidity (RH) and saturation vapor pressure of the air (p_{ws}), as shown in Equation 1 (Sabeh 2020):

$$VPD = p_{ws} \times (1 - \frac{RH}{100})$$

Equation 1

p_{ws} is calculated from the dry-bulb temperature (T) of air according to Equation 2 below (ASHRAE 2009):

$$\ln(p_{ws}) = \frac{C_8}{T} + C_9 + C_{10} \times T + C_{11} \times T^2 + C_{12} \times T^3 + C_{13} \times \ln(T)$$

Equation 2

In Equation 2, C_8-C_{13} are constants (ASHRAE 2009).

State-of-the-Art Dehumidification Approaches

General approaches to dehumidification and cooling for indoor farms rely on refrigerant-based coils and fully recirculated air. Although outside air-side economizers could offer efficient cooling, they are typically avoided to limit pest and pathogen infiltration to the grow space and to maintain injected carbon dioxide (CO_2) for plant growth. Below, we describe four cooling and dehumidification approaches for 100 percent recirculated air, including the retrofit system (conventional air

conditioning with heat recovery heat exchanger). This study is a side-by-side comparison of conventional air conditioning with electric resistance reheat to the retrofit system.

Conventional Air Conditioning with Electric Resistance or Gas Reheat

Conventional HVAC systems are often inefficient when applied to indoor farming. To dehumidify, these systems cool air to its dewpoint at the evaporator coil so that moisture condenses. However, achieving the necessary dehumidification in this way makes the supply air too cold for the plants. To counteract this over-cooling, electric resistance or gas heat is used to reheat the air before it is supplied back to the farm. Figure 1a below shows the components involved and the airflow path in this approach. Both container farms involved in this field demonstration were initially equipped with the electric resistance reheat approach.

Conventional Air Conditioning with Stand-Alone Dehumidifiers

Another conventional approach is to place stand-alone, high-efficiency dehumidifiers directly inside the grow space to handle the latent cooling load while a separate air conditioning system handles the sensible cooling load (Figure 1b). The dehumidifiers remove moisture from the air but reject heat into the space. Using multiple pieces of HVAC equipment to meet the cooling load is inherently inefficient, as each system has its own fans and compressor. In addition, the heat rejected by the dehumidifiers increases the load on the air conditioner. However, the combination of dehumidifiers and air conditioners can result in an appropriate sensible heat ratio (SHR), or the ratio of sensible cooling to total cooling—which includes moisture removal—so that the space is not over-cooled and does not require reheat.

Conventional Air Conditioning with Condenser Air Heat Recovery

A more efficient option for HVAC in indoor farms is to use a standard air conditioning system with reheat provided by heat recovery from the condenser (Figure 1c). In this configuration, the refrigeration system includes two condensers: a hot-gas reheat condenser and a conventional outdoor air-cooled condenser. A modulating reheat valve adjusts how much recovered heat is directed to rewarm the supply air delivered to the grow space. While there is still an efficiency penalty—the compressor must remove heat only to add some of it back—this approach is more efficient than electric or gas reheat. The tradeoff is the added cost and complexity of the refrigeration system.

Conventional Air Conditioning with Heat Recovery Heat Exchanger

An alternative approach to dehumidification for an indoor farm is conventional air conditioning paired with a heat recovery heat exchanger, which this study evaluated. This approach couples a traditional air handling unit (AHU) with a plate air-to-air heat exchanger (Figure 1d). The heat exchanger transfers sensible heat from the return air to the supply air, effectively pre-cooling the return air close to its dewpoint before it reaches the evaporator coil. This also reduces the amount of reheat energy that must be added back to the supply air. The evaporator cooling energy is then primarily used for dehumidification as opposed to sensible cooling.

Since the latent load is typically dominant in indoor farms, the resulting SHR is well-suited to an indoor growing application. The AHU is equipped with a variable speed fan, which enables some control of the SHR; previous laboratory testing demonstrated that increasing airflow rate increases the SHR from 0.10 to 0.25 (Ross, McMurry and Pistochini 2016). A secondary “trim” cooling coil for

the supply air can be added to increase control and additional capacity, which increases both cost and space required for equipment. For this project, we evaluated the performance of this approach without a trim cooling coil, as shown in Figure 1d.

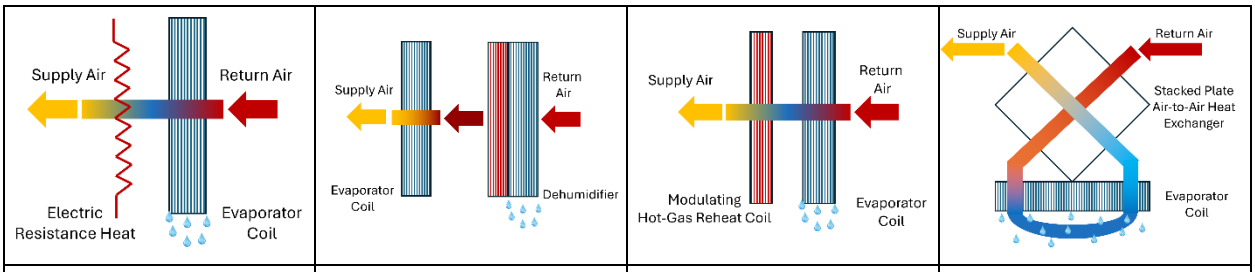

a: Conventional air conditioning with electric resistance reheat	b: Conventional air conditioning with stand-alone dehumidifiers	c: Conventional air conditioning with modulating hot-gas reheat	d: Conventional air conditioning with heat recovery heat exchanger

Figure 1: Diagrams of HVAC approaches for indoor farming.

Previous Research

In 2016, the Western Cooling Efficiency Center (WCEC) conducted a laboratory study of the retrofit system. The latent and sensible cooling performance was measured for two different indoor conditions (80°F/69.5°F dry-bulb/wet-bulb and 75°F/62.4°F dry-bulb/wet-bulb) across a range of flow rates and outdoor air conditions. The retrofit system was instrumented with a sensing and data acquisition system, and for each test condition, the team determined the total capacity, Coefficient of Performance (COP), dehumidification capacity, latent COP, dehumidification efficiency, and SHR. The WCEC used the measured data to create a model of an indoor farm comparing energy use when equipped with conventional air conditioning with stand-alone dehumidifiers versus the retrofit system. The model was applied to Los Angeles, Oakland, and Sacramento, as well as several cities in Colorado. For the California cities, the model showed 35 percent to 65 percent energy savings, depending on the internal loads.

Objectives

This field demonstration evaluated the energy consumption and operational viability of the retrofit system—an all-electric dehumidification and cooling system—installed in an operational indoor container farm. The project conducted a side-by-side comparison between the retrofit system and a conventional air conditioning system with electric resistance reheat in two farms that grow lettuce.

The main research questions driving this study were:

- What energy savings and demand reduction can be achieved using the retrofit system compared to a conventional air conditioning system with electric resistance reheat?
- How well does the retrofit system manage sensible and latent loads under real-world growing conditions?
- Do the field results align with previously conducted laboratory testing?

Throughout this study, the team:

- Documented the installation, operational experience, and maintenance needs of the retrofit system and collected feedback from the indoor farm operators.
- Quantified the energy demand, energy use, sensible cooling and dehumidification capacity of both systems.
- Compared field results to previously obtained laboratory test results and a model that was developed from the laboratory test data.

To support technology transfer, results will be shared through:

- Industry events and conference presentations.
- Direct engagement with investor-owned utilities and consultants, CalNEXT partners, equipment manufacturers, container farm manufacturers, equipment distributors, and engineering firms evaluating custom measure development.

Methodology and Approach

This project was a field demonstration of the retrofit system's real-world performance relative to that of a conventional approach. As such, our methodology included identifying a suitable test site to conduct a side-by-side study, instrumenting the test site to collect data on baseline operation, retrofitting the test site with the novel HVAC system and adjusting the instrumentation as needed, and observing the retrofit system's performance relative to a baseline.

Test Site(s)

The site consists of two container farms, both owned and operated by the nutrition department of a school district in California's Climate Zone 4. Located at two different schools within the same city, the farms are referred to as "Farm 1" (installed in October 2021) and "Farm 2" (installed in November 2022). The two farms are about four miles apart from each other, so they are expected to experience similar weather. However, there are deciduous trees on the south and west exposures that shade Farm 2, so the radiant heat loads on Farm 2 in summer and shoulder seasons are presumed to be lower than the radiant heat loads on Farm 1. The test site was chosen due to its location within Pacific Gas and Electric Company service area, the presence of two container farms (allowing for one control and one retrofit HVAC system to operate with comparable loads and comparable weather), and the support of the school district. The farms are used year-round to grow lettuce—which is served to students through the school lunch program—and are managed by a staff member from the nutrition department, who regularly starts new lettuce crops from seed.

Each 298-square-foot container farm includes a 7.5-foot-long nursery section that holds up to 16 seedling trays, with red and blue grow lights positioned above each shelf (Figure 2). At the rear of the container are two double-sided, 30-foot-long plant cultivation panels, which are suspended from ceiling-mounted tracks. Red and blue grow lights are also mounted on the side walls and on both sides of a central, track-mounted lighting panel positioned between the plant cultivation panels. Both the plant panels and the lighting panel can slide laterally along the tracks, allowing access throughout the farm. This layout creates four active growing faces, each illuminated by a lighting

panel. Lettuce is grown hydroponically in vertical strips of inert reticulated foam, irrigated by drip emitters at the top of each strip. Condensate from the HVAC system is captured and returned to a water reservoir at the rear of the farm, minimizing water loss to the environment aside from plant uptake. The total growing area for each container farm is equivalent to approximately 3,000 linear feet, or about 2.5 acres of conventional farmland.

Both farms grew five varieties of lettuce throughout the entire study. The lettuce growing cycle spans seven weeks: three weeks in the nursery section followed by four weeks on the main plant cultivation panels. Planting on the main panels is staggered across four phases between the two container farms, allowing for a continuous weekly harvest of approximately 2,000 fully mature lettuce plants.

Figure 2: Container farm nursery area (left), cultivation walls, and lighting panels (right).

The grow lights in the farm are the primary load on the HVAC system, as they add sensible heat to the space and drive transpiration in the lettuce. They are programmed to operate on a 24-hour cycle, with 18 hours of "day," where the grow lights are on, followed by 6 hours of "night," where the grow lights are off. Generally, both farms followed the lighting schedules shown in Figure 3 throughout the entire study. During the day period, the lighting schedule provided 3 hours of blue light (1.8 kilowatts (kW)), 10 hours of combined red and blue light (5.1 kW), and 5 hours of red light (3.3 kW). The lighting schedule does not observe local time changes, so the start and end times of each lighting stage differ by one hour in standard time and daylight saving time. The team observed that sometimes the day period began later than scheduled due to the farm operators working inside the farm during scheduled daytime and manually shutting off the lights. However, these disruptions were rare and typically did not postpone the day period by more than one hour.

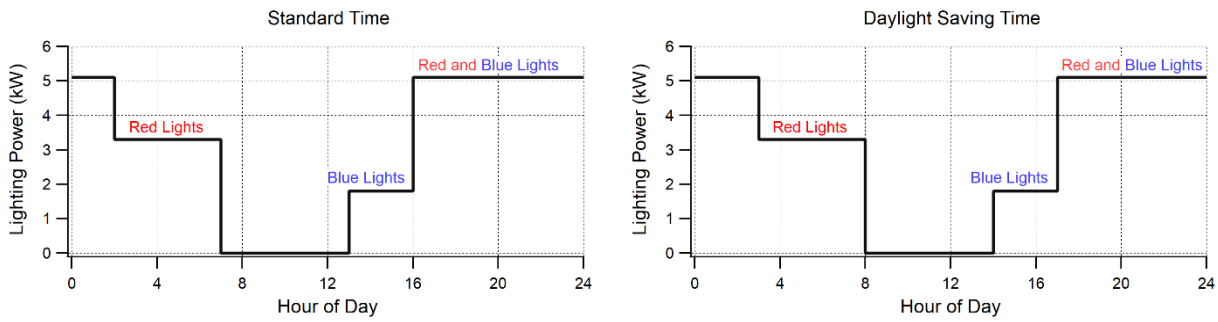

Figure 3: Grow light schedule observed in both farms during standard time (left) and daylight saving time (right).

Baseline HVAC System

Both farms were initially equipped with a 3-ton packaged HVAC system, which was mounted on the side of the container. The packaged system consisted of a standard direct expansion R-410A refrigeration system with electric resistance reheat rated at 9 kW. A thermostat located at the back of the farm controlled a set of relays that switched cooling (cooling compressor only), dehumidification (cooling compressor plus electric resistance reheat), and heat (electric resistance reheat only). A separate relay controlled the HVAC system indoor fan, which ran continuously at a fixed speed—with a volumetric flow rate of approximately 850 cubic feet per minute (CFM)—to circulate the air inside the container. The return air entered the HVAC system through a duct located at the back of the farm, and the conditioned supply air was delivered to the front of the farm through a supply duct located beneath the farm's floor. Figure 4 below depicts the layout of the farm and baseline HVAC system. The performance of each farm's baseline HVAC system was monitored from December 14, 2024, through May 31, 2025, as described in the Baseline Instrumentation section.

At the recommendation of container farm manufacturer, the farm operator programmed the indoor temperature to 69°F during the day period and 65°F during the night period. The indoor RH setpoint was 70 percent for both day and night; these setpoints equate to a VPD setpoint of 0.73 kPa with lights on and 0.63 kPa with lights off.

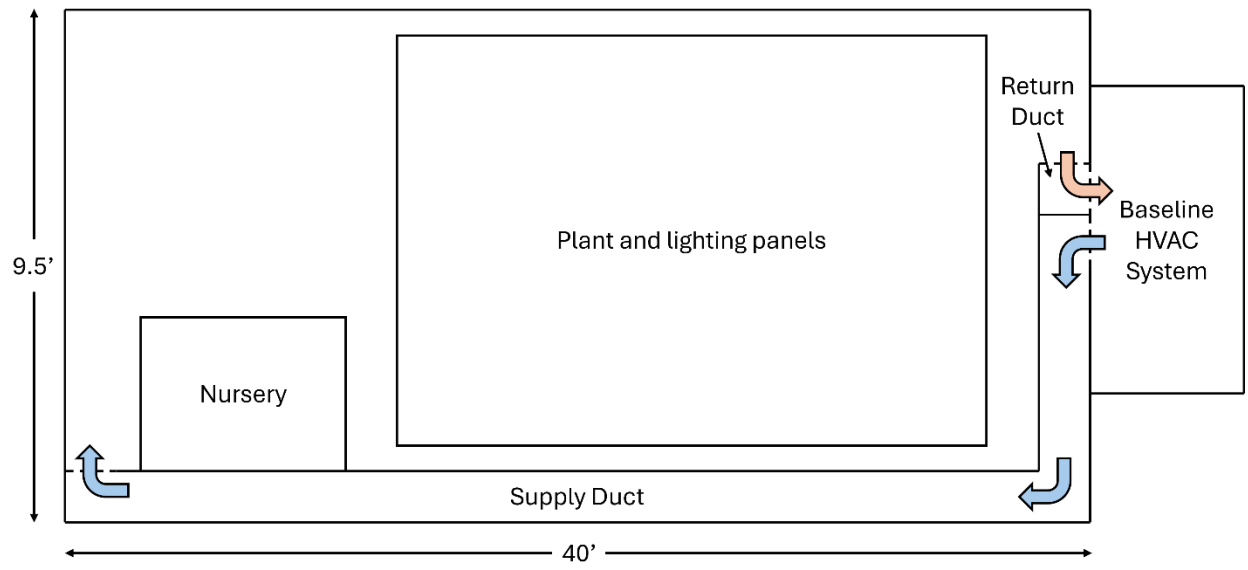

Figure 4: Side view of farm interior and baseline HVAC system.

Test Plan

After identifying a test site, our test plan consisted of instrumenting both farms with a sensing and data acquisition system, monitoring the baseline operation of both farms, replacing one farm's baseline HVAC equipment with the retrofit system, observing the performance of the retrofit system relative to the baseline, and making adjustments to the retrofit as needed.

Baseline Instrumentation and Monitoring

In December 2024, the team instrumented both farms with the sensors listed in Table 1 and shown in Figure 5 and Figure 6. Air temperature and RH were measured entering the HVAC system (return air), after the cooling coil but before the reheat coil (pre-reheat), leaving the HVAC system (supply air, floor duct entrance), and entering the container after passing through the 40-foot underfloor supply duct (supply air, floor duct exit). We measured power draw and electricity consumed separately for the farm grow lights, HVAC compressor, HVAC indoor fan, and HVAC electric resistance heater. Total HVAC power and energy consumption were also metered, which consisted of the sum of the compressor, indoor fan, electric resistance heater, condenser fan, and any ancillary controls. Finally, a carbon dioxide (CO_2) sensor measured the CO_2 levels inside the farm.

We sampled analog output voltages from the temperature, RH, and CO_2 sensors with a ThermoFisher Scientific dataTaker DT85M Series 3 data logger. Analog data were sampled six times per minute, averaged, and logged once per minute. Additionally, power, voltage, current, and power factor readings from each power meter—which transmit data over a serial communication protocol—were sampled six times per minute, averaged, and logged once per minute. Every day at midnight, the data stored locally on the dataTaker uploaded to an online file server via a cellular network, where we remotely retrieved the data files. The team monitored the baseline operation of both farms through May 2025.

Table 1: Instrumentation of baseline HVAC system.

Symbol	Measurement	Manufacturer and Model Number	Reported Accuracy
T_{SA}	Supply air temperature, floor duct entrance	Vaisala HMP110	±0.36°F
RH_{SA}	Supply air relative humidity, floor duct entrance	Vaisala HMP110	±1.5%
T_{SA2}	Supply air temperature, floor duct exit	Vaisala HMP110	±0.36°F
RH_{SA2}	Supply air relative humidity, floor duct exit	Vaisala HMP110	±1.5%
T_{RA}	Return air temperature	Vaisala HMP110	±0.36°F
RH_{RA}	Return air relative humidity	Vaisala HMP110	±1.5%
T_{OA}	Outdoor air temperature	Vaisala HMP110	±0.36°F
RH_{OA}	Outdoor air relative humidity	Vaisala HMP110	±1.5%
T_{PH}	Supply air temperature pre-reheat	Vaisala HMP110	±0.36°F
RH_{PH}	Supply air temperature pre-reheat	Vaisala HMP110	±1.5%
P_L	Power draw of farm grow lights	DENT PowerScout 3+	±0.2%
P_C	Power draw of compressor	DENT PowerScout 3+	±0.2%
P_F	Power draw of indoor fan	DENT PowerScout 3+	±0.2%
P_H	Power draw of electric resistance heater	DENT PowerScout 3+	±0.2%
P_{TOT}	Power draw of total HVAC system	DENT PowerScout 3+	±0.2%
CO_2	Carbon dioxide concentration	Senseair tSENSE 070-8-0001	±30 ppm ±3% measurement

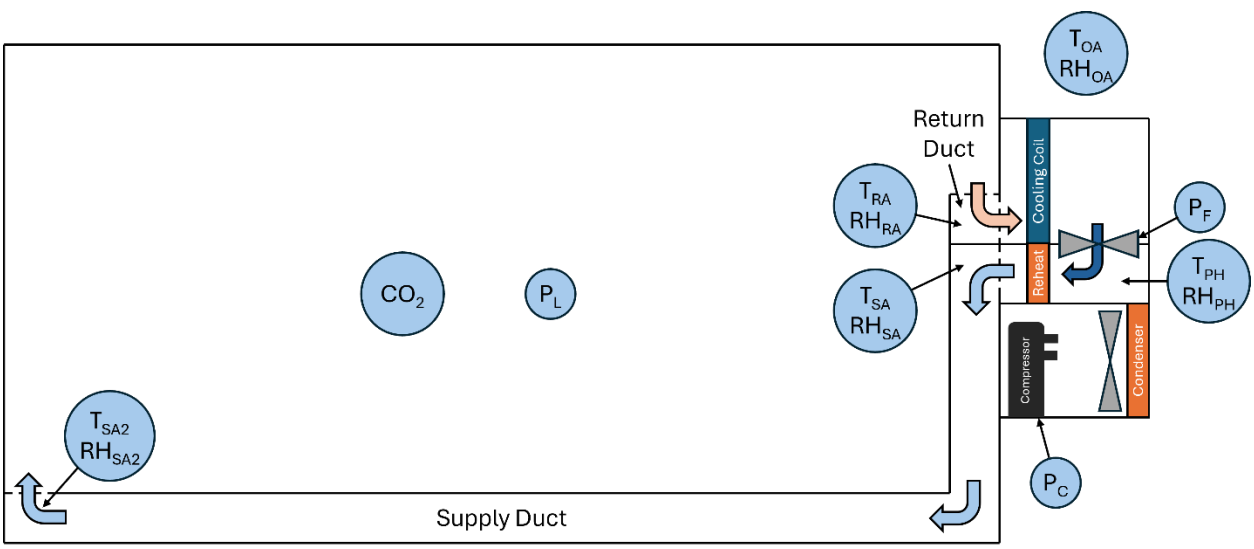

Figure 5: Diagram showing sensor locations inside farm and baseline HVAC system.

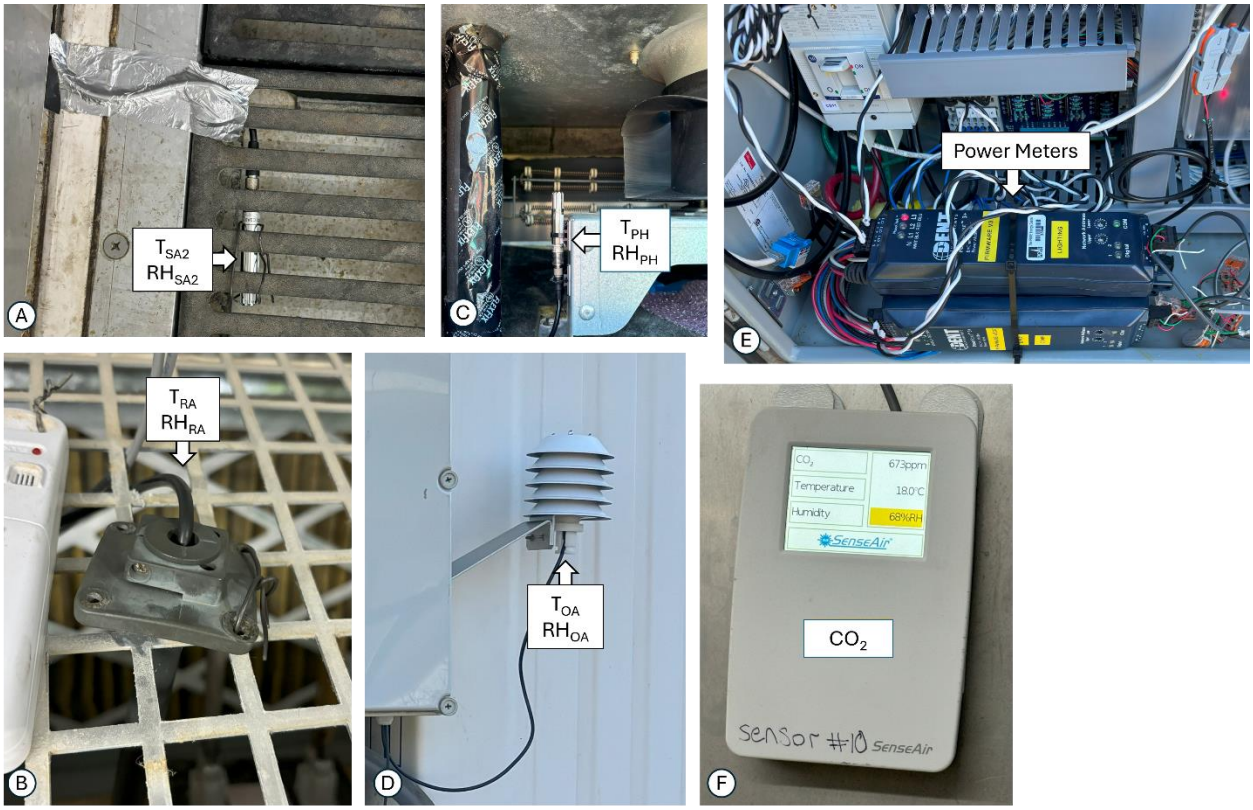

Figure 6: Instrumentation installed to monitor the baseline HVAC systems at both farms.

HVAC Retrofit

In July 2025, we replaced Farm 1's HVAC system with the retrofit system. The AHU contained the evaporator coil, air-to-air plate heat exchanger, and indoor evaporator fan. The retrofit system's supply and return did not align with the farm, so it was installed on the ground offset from the farm (Figure 7). Ductwork with R-8 insulation was installed to connect the retrofit system's supply and return to the farm. The evaporator coil in the AHU was field-connected to a 2.5-ton condensing unit. An electric resistance heater, rated at 2 kW, was installed in the ductwork after the AHU exit to provide some heating capacity, particularly for winter months when the grow lights are off.

It is possible to redesign the geometry of the retrofit system and/or the container farm to mount the AHU on the side of the container, which could significantly reduce or eliminate the need for ducting. However, due to time and budget constraints, the team did not pursue that approach in this project. The primary goal was to assess energy savings within time and budget constraints, necessitating the approach of placing the retrofit system on the ground; however, this retrofit was still costly, and to be feasible for widespread adoption, the geometry of the retrofit system would need to be redesigned to integrate seamlessly into the farm. This would also save space, which is crucial for farms located in urban, space-limited sites. The research team has engaged both the manufacturer of the retrofit system and the manufacturer of the container farm and all parties seem open to possible future integration solutions.

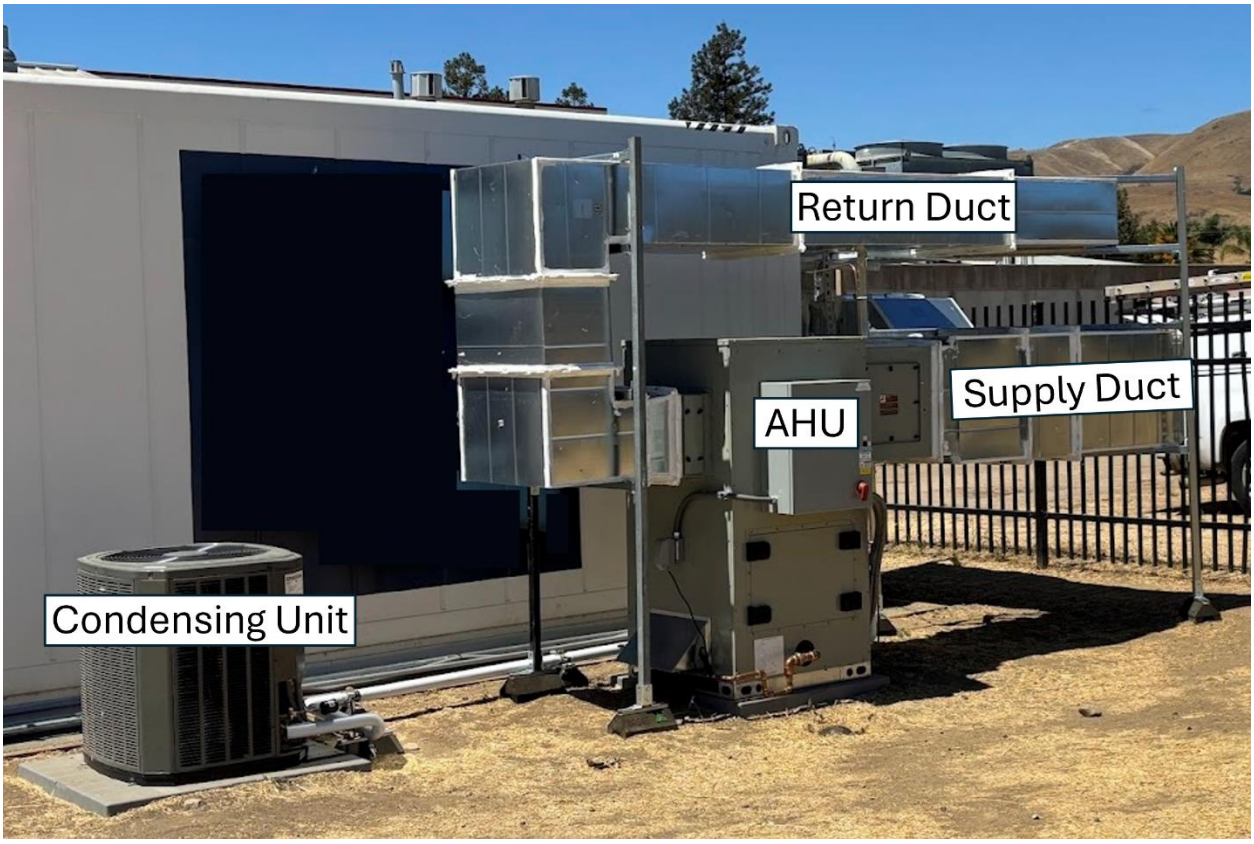

Figure 7: The retrofit system system installed at Farm 1.

Retrofit Instrumentation and Monitoring

To account for differences between the baseline and retrofit HVAC systems, the team modified the instrumentation at Farm 1 following the retrofit. We moved the pre-reheat T/RH sensor to the corresponding location on the retrofit system (Figure 8) and installed a new T/RH sensor at the end of the return air duct at the inlet to the AHU (Table 2). The T/RH sensors monitoring the return air, supply air at the floor duct exit, and outdoor air were not disturbed.

The team did not alter the power meter that monitored the grow lights, but we did modify the power meters that previously tracked the indoor fan, compressor, heater, and total system on the baseline HVAC system to monitor the following variables:

- Power draw of the condensing unit (compressor and condenser fan) (P_C)
- Power draw of the retrofit system AHU (indoor fan, heater, and ancillary controls) (P_{AHU})
- Power draw of the electric resistance heater (P_H)

Total HVAC power draw (P_{TOT}) and energy use were aggregated as the sum of the power draw/energy use of the retrofit system AHU and the condensing unit. Additionally, we logged the outputs from the retrofit system's controller to track the system operating mode.

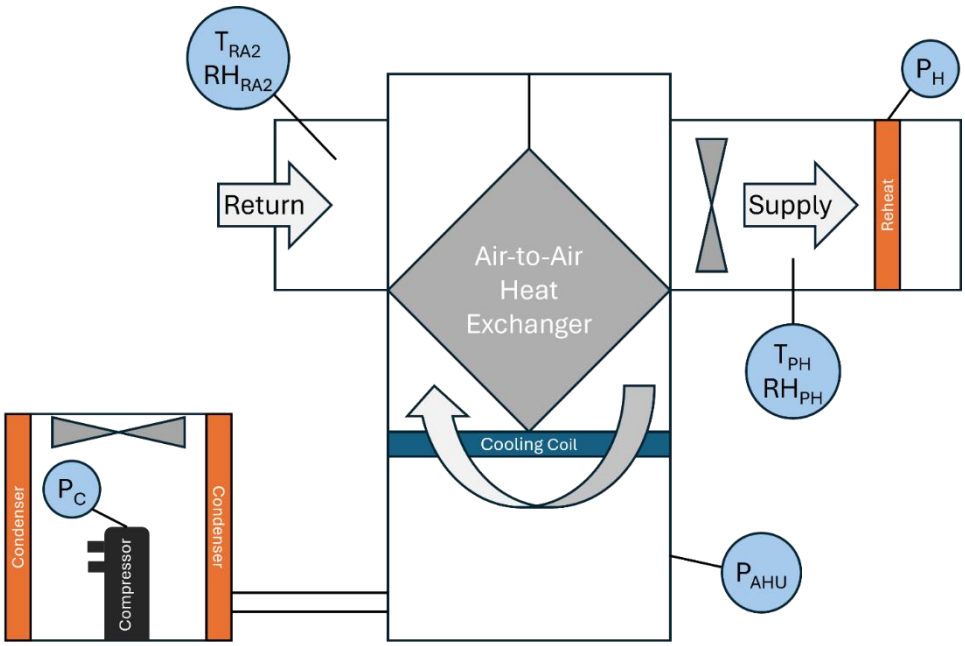

Figure 8: Sensor locations in the retrofit system.

Table 2: Sensors added during the retrofit.

Symbol	Measurement	Manufacturer and Model Number	Reported Accuracy
T_{RA2}	Return air temperature, duct exit	Vaisala HMP110	±0.36°F
RH_{RA2}	Return air relative humidity, duct exit	Vaisala HMP110	±1.5%

Low-Ambient Cooling

Unlike residential cooling systems, HVAC systems serving indoor farms run continuously throughout the day and the year. During the night and the winter, when ambient temperatures are low, the refrigerant temperature in the evaporator can drop below 32°F. This can lead to ice formation on the evaporator coil, which inhibits heat transfer from the air to the refrigerant. If insufficient heat is transferred to the refrigerant, the refrigerant may not fully evaporate in the evaporator, causing some refrigerant to return to the compressor in the liquid phase. This can severely damage the compressor.

To protect the compressor, the system was designed with the following features:

- Evaporator defrost control switch (model AY28X079), which shuts off the compressor when the evaporator coil temperature drops below freezing.
- Low ambient head pressure control kit (model BAYLOAM107A), which cycles the condenser fan to maintain the refrigerant liquid line temperature to a setpoint.
- Crankcase heater, which warms the base of the compressor when the refrigerant discharge line temperature is below a setpoint.

After the initial retrofit, the team observed that the new HVAC system met the dehumidification requirements of the farm but struggled to meet the sensible cooling requirements. We theorized that the low-ambient head pressure control kit, which ensures that the refrigerant does not get too cold but reduces the sensible cooling capacity, made it more difficult to meet the desired indoor conditions. While working on a long-term solution to improve sensible cooling (described in the Partial Heat Exchanger Air Bypass section), we disconnected the head pressure control kit, which we suspect eventually led to compressor damage. In November 2025, we replaced the compressor and discovered that the system had shipped with a factory-installed orifice plate for refrigerant management instead of a thermostatic expansion valve (TXV), which is required for low-ambient operation. Thus, during the compressor replacement we also removed the orifice plate and installed a TXV. After the compressor replacement and TXV installation, the team recharged the system with new refrigerant and connected the low-ambient control components.

The system operated with the low-ambient kits and TXV for the remainder of the study, but in June 2026, the system's cooling capacity began declining. A site visit confirmed that the compressor was failing, and we replaced it on July 6, 2026. The cause of this failure is undetermined, but one possibility is that frequent compressor cycling during the winter (which can reach 150 cycles per day) caused the failure. This frequent cycling could easily be reduced by an increase in the deadband for the humidity control of the farm, but it is unclear at this time if that would resolve the problem. We have engaged the compressor distributor to explore the cause of the compressor failures and propose potential solutions.

Partial Heat Exchanger Air Bypass

Preliminary performance results showed that the retrofit system was providing too much dehumidification and not enough sensible cooling, especially when grow lights were on and lettuce plants were small (see Indoor Air Conditions). To address this problem, we designed and field-installed a partial bypass of the plate heat exchanger that funneled a portion of the return air directly beneath the evaporator coil (Figure 9 and Figure 10). This portion of the return air is not pre-cooled by the plate heat exchanger, so it receives primarily sensible cooling and minimal dehumidification when it passes through the evaporator. This increases the overall sensible cooling capacity of the system.

The team installed the partial heat exchanger air bypass in November 2025 when we replaced the compressor. The bypass consists of a duct that connects the return duct to the space beneath the evaporator coil, a switchable damper, and a filter box to filter the bypass air (since it bypasses the main filter). With the damper open, the airflow through the bypass was 176 CFM at low speed and 281 CFM at high speed, which equates to approximately 20 percent of the total airflow at either speed.

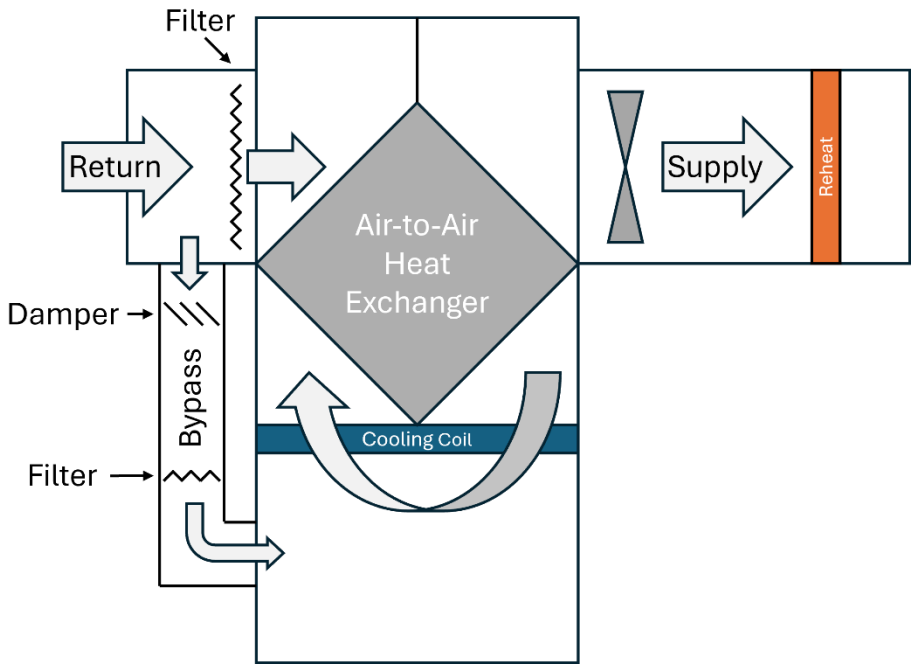

Figure 9: Diagram of airflow through the retrofit system with the partial heat exchanger bypass installed.

Figure 10: Partial heat exchanger bypass return duct connection with damper (left) and AHU connection with filter box (right).

Original Retrofit HVAC Control System

The team used the original HVAC control algorithm and existing relays, as well as a new programmable logic controller (PLC), to control the retrofit system. Based on the indoor temperature (T) and RH, the original HVAC control algorithm switched three relays: the fan relay enabled the indoor fan, the cooling relay enabled the condensing unit, and the heating relay enabled the electric heater (Figure 11). Because the indoor fan is variable speed, the PLC provided the required 0 volt (V) to 10 V signal for fan speed control.

We added a current transducer to the grow light circuit to determine whether the lights were on or off and feed this status to the PLC, which then selected low or high fan speed based on HVAC relay status and lighting operation. When there was a call for cooling and the grow lights were on, the fan operated at 7.8 V (approximately 1,490 CFM); otherwise, the fan operated at 5 V (approximately 830 CFM). The higher fan speed was intended to increase total cooling capacity and SHR during periods of peak sensible load caused by the grow lights.

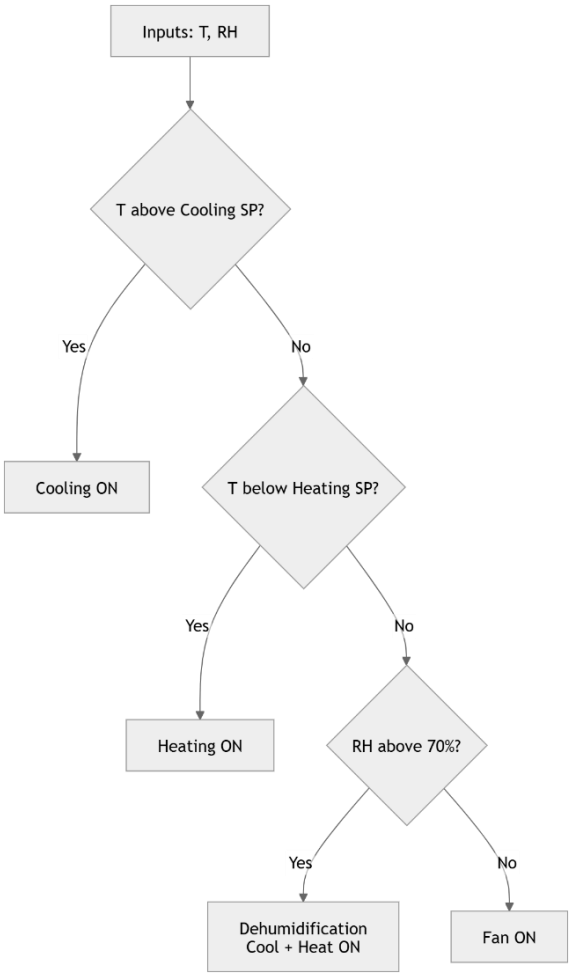

Figure 11: Original retrofit control system algorithm.

As shown in Figure 11, the original control algorithm prioritized meeting the temperature setpoint first. Dehumidification was the lower priority, only activating dehumidification (cooling and heat) when the temperature was in range and the RH was greater than 70 percent. This approach was appropriate for the baseline HVAC system, which must provide reheat when dehumidifying. However, for the retrofit system (which can dehumidify without overcooling), it resulted in unnecessary reheat during dehumidification, since heating was applied even when the space was already within the heating setpoint range.

Original Retrofit HVAC Control System with Bypass

After the installation of the bypass, the team updated the PLC to open the bypass when there was a "Cooling ON" call and the grow lights were on, as indicated by the current transducer. This improved the system's ability to meet the cooling setpoint during the peak sensible load.

Improved Retrofit HVAC Control System with Bypass

With the support of the container farm manufacturer, the team updated the cloud-based control algorithm to reduce unnecessary reheat during dehumidification (Figure 12) by changing the controls so that the reheat did not run when the temperature of the farm was above the heating setpoint. To prevent the farm from getting too cold (since heating capacity was limited), we increased the heating setpoint from 55°F to 58°F. We also reconfigured the PLC to run the fan at high speed whenever cooling was on, regardless of the status of the grow lights.

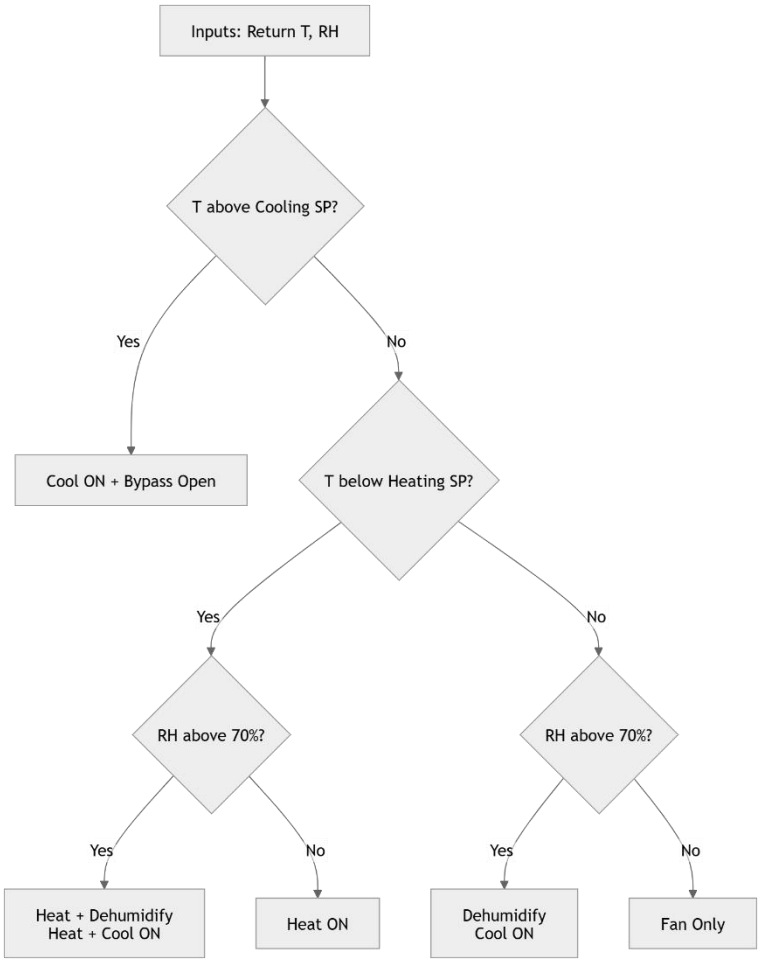

Figure 12: Improved retrofit control system algorithm.

Calculation Methods: HVAC Modes

The baseline HVAC system had four modes: fan, cool, dehumidify + reheat, and heat (Table 3). We post-processed the power data to disaggregate baseline HVAC operation mode. As shown in Table 3, the baseline system achieved dehumidification by operating the cooling system with electric reheat.

For the retrofit system, the team post-processed the controller outputs to determine the operation mode. Under the improved control algorithm implemented at the start of Period 4, the retrofit system operated with five distinct modes: fan, cool, dehumidify, dehumidify + reheat, and heat (Table 4). A major benefit of the retrofit system is that it can operate in dehumidify mode without using electric reheat due to the heat recovery by the air-to-air heat exchanger. As a result, the retrofit system had both dehumidify and dehumidify + reheat modes.

Table 3: Operating modes for baseline HVAC.

Mode	Fan Status	Compressor Cooling Status	Electric Heat Status
Fan	On	Off	Off
Cool	On	On	Off
Dehumidify + Reheat	On	On	On
Heat	On	Off	On

Table 4: Operating modes for the retrofit system.

Mode	Fan Status	Compressor Cooling Status	Electric Heat Status	Bypass Status
Fan	On – low	Off	Off	Closed
Cool	On – high	On	Off	Open
Dehumidify	On – low	On	Off	Closed
Dehumidify + Reheat	On – low	On	On	Closed
Heat	On – low	Off	On	Closed

Calculation Methods: Cooling Capacity and Efficiency

The rate at which an HVAC system removes heat is the system's total cooling capacity, where heat removal includes both the reduction of the air's dry-bulb temperature (sensible cooling) and the removal of moisture (latent cooling). The total capacity—measured in kilo-British thermal units per hour (kBTU/h)—is equal to the product of the mass flow rate of air through the HVAC system and the difference in air enthalpy across the HVAC system. The enthalpy of air is calculated from the dry-bulb temperature and humidity ratio of air according to Equation 3 below (ASHRAE 2009).

$$h = 0.240 \times T + W \times (1061 + 0.444 \times T)$$

Equation 3

In Equation 3, h is the enthalpy of air, T is the dry-bulb temperature of air, and W is the humidity ratio of air. For each HVAC system, the total cooling capacity was calculated from the difference in enthalpy between the return air (RA) and the pre-reheat (PH) air, as shown in Equation 4:

$$\dot{Q}_{Cooling,\ Total} = \dot{m} \times (h_{RA} - h_{PH})$$

Equation 4

In Equation 4, $\dot{Q}$ is the total cooling capacity, $\dot{m}$ is the mass flow rate of air through the system, and h is the enthalpy of the air at the specified location. For the retrofit system, the team measured RA conditions using sensor RA2 so that any duct losses were not included. For the baseline HVAC system, we only calculated cooling capacity for the cool mode. For the retrofit system, we calculated cooling capacity for both the cool mode and the dehumidify mode, since both modes used only the cooling coil with no electric reheat.

The team calculated the sensible cooling capacity of each HVAC system from the product of the mass flow rate of air through the HVAC system, the specific heat of air (C_P, a property of air), and the temperature change across the HVAC system, as shown in Equation 5:

$$\dot{Q}_{Cooling,\ Sensible} = \dot{m} \times C_P \times (T_{RA} - T_{PH}) \quad [5]$$

Equation 5

The latent cooling capacity for both systems was calculated as the difference between the total cooling capacity and sensible cooling capacity, according to Equation 6 below:

$$\dot{Q}_{Cooling,\ Latent} = \dot{Q}_{Cooling,\ Total} - \dot{Q}_{Cooling,\ Sensible} \quad [6]$$

Equation 6

The SHR was calculated from Equation 7:

$$SHR = \dot{Q}_{Cooling,\ Sensible} / \dot{Q}_{Cooling,\ Total} \quad [7]$$

Equation 7

The COP of an HVAC system is a common metric of HVAC efficiency; it is the ratio of heat removed by the HVAC system to the power draw of the HVAC system. The COP for both the baseline and retrofit systems was calculated according to Equation 8 below:

$$COP = \frac{\dot{Q}_{Cooling.\ Total}}{P_{TOT}} \quad [8]$$

Equation 8

Calculation Methods: Dehumidification + Reheat Capacity

To prevent overcooling of the farm, the baseline HVAC system—and, at times, the retrofit system—must operate in the dehumidify + reheat mode, where the cooling coil runs simultaneously with electric reheat to remove moisture while maintaining the required indoor air temperature and VPD. This operating mode is expected to occur less frequently with the retrofit system because heat is recovered through the plate heat exchanger, preventing overcooling. For each system, the total

dehumidify + reheat capacity was calculated by subtracting the power of the electric heater (P_H) from the calculated total cooling capacity, as show in Equation 9:

$$\dot{Q}_{Dehumidify+Reheat,\ Total} = \dot{Q}_{Cooling,\ Total} - P_H \quad [9]$$

Equation 9

Similarly, the sensible dehumidify + reheat capacity was calculated by subtracting the heater power draw from the calculated sensible cooling capacity, as shown in Equation 10. This is because the heater only raised the dry-bulb temperature of the supply air and did not remove or add moisture.

$$\dot{Q}_{Dehumidify+Reheat,\ Sensible} = \dot{Q}_{Cooling,\ Sensible} - P_H \quad [10]$$

Equation 10

The latent capacity in this mode was calculated by subtracting the sensible dehumidify + reheat capacity from the total dehumidify + reheat capacity, as shown by Equation 11:

$$\dot{Q}_{Dehumidify+Reheat,\ Latent} = \dot{Q}_{Dehumidify+Reheat,\ Total} - \dot{Q}_{Dehumidify+Reheat,\ Sensible} \quad [11]$$

Equation 11

Finally, COP for this mode was calculated according to Equation 12:

$$COP = \frac{\dot{Q}_{Dehumidify+Reheat}}{P_{TOT}} \quad [12]$$

Equation 12

Findings

Overview

In this section, we first present results for the retrofit system versus the baseline farm for indoor conditions, average daily total energy use, and average daily energy use during peak hours. The results were divided into four operational periods to reflect successive improvements to the retrofit system installation at Farm 1, while Farm 2 continued operating with the baseline HVAC system throughout the study as a comparison site (Table 5). Periods 2 through 4 represent successive post-retrofit phases corresponding to initial operation of the retrofit system (Period 2), operation of the retrofit system with the bypass (Period 3), and operation of the retrofit system with the bypass and improved controls (Period 4). Across all periods, the team excluded days with incomplete data from the analysis to ensure consistency between farms and maintain a dataset consisting only of complete operational days. Note that the monitoring periods were not designed to be of equal duration or to have similar weather, as improvements were implemented as quickly as possible to achieve satisfactory indoor conditions with the retrofit system. The primary goal was not to evaluate the incremental benefits of each individual improvement in detail, but rather to achieve a well-performing installation as rapidly as possible. For completeness, we include summary indoor

condition and energy performance data for each version of the retrofit installation. For each period, we compared indoor conditions and HVAC energy use between farms, as each farm experienced similar weather and loads within the same period.

We also compared indoor conditions and HVAC energy use between Farm 1 in Period 1, when Farm 1 was equipped with the baseline equipment, and Farm 1 in Period 4, when Farm 1 was equipped with the finalized retrofit installation. Period 1 and Period 4 spanned the same months of the year and had similar weather; the outdoor air temperature at Farm 1 was 54.7 ± 11.1 °F (mean ± one standard deviation) in Period 1 and 57.5 ± 10.5 °F in Period 4. This allowed us to compare the retrofit system to the baseline equipment without any confounding differences between Farm 1 and Farm 2. We also developed curves to predict daily HVAC energy use of both the baseline and retrofit systems based daily average outdoor air temperature. Using typical meteorological year (TMY) weather data for the location of the demonstration site, we forecasted the annual savings attributable to the retrofit system.

There are two aspects of HVAC energy consumption in the indoor farm that are sensitive to weather. First, the sensible capacity, latent capacity, and efficiency of the refrigeration system are expected to increase as outdoor air temperature decreases. Therefore, for the final refined retrofit installation relative to the baseline installation (Period 4), we present more detailed results on HVAC system performance as a function of outdoor weather conditions. To the extent possible, these results were compared to laboratory test data collected in 2016 (Ross, McMurry and Pistochini 2016).

Second, the heat gain or loss through the farm envelope is influenced by weather conditions, with outside air temperature and solar radiation expected to have the greatest impact. Accordingly, we analyzed the heat gain to the farm as a function of outdoor air temperature. We also analyzed dehumidification rates, which reflect the transpiration rates of the lettuce, and compared these results to a simple indoor farm model developed in 2016 as part of the laboratory testing.

Finally, we developed simplified performance models for each HVAC system (the retrofit system versus baseline) and quantified the sensible and latent indoor farm loads. These inputs can be combined with TMY weather for California climate zones to forecast the impact of the retrofit system versus the baseline in reducing total and on-peak energy use for a container farm that grows lettuce.

Table 5: Time periods, date ranges, and operating conditions.

Period	Date Range	Excluded Dates	# Days	Condition
1	12/14/2024 to 05/31/2025	12/26/2024 02/13/2025 02/17/2025 03/31/2025	165	Farm 1: baseline Farm 2: baseline
2	08/14/2025 to 11/11/2025	09/23-09/25/2025 10/13/2025 10/23–10/24/2025	84	Farm 1: retrofit Farm 2: baseline

3	11/20/2025 to 01/05/2026	12/17/2025 12/19–12/21/2005	43	Farm1: retrofit + bypass Farm 2: baseline
4	01/07/2026 to 05/07/2026	01/28/2026 02/02/2026 02/16/2026 02/18/2026 02/22/2026 02/27/2026	115	Farm 1: retrofit + bypass + improved controls Farm 2: baseline

Results: All Monitoring Periods

Average Daily Lighting Energy Use

The average daily lighting energy use was consistent across both farms and all periods, as shown in Table 6. Variations in daily lighting energy use are attributed to the farm operator temporarily turning the lights off during scheduled "daytime" to perform farm tasks. The grow lights are the primary internal load in the farm—they add heat directly to the space and drive transpiration in the lettuce, which adds humidity. The average daily lighting energy use was approximately 3 percent higher in Farm 1, potentially due to its slightly older and possibly less efficient lighting system.

Table 6: Lighting energy use at each farm across all periods.

Period	Farm 1 Lighting Energy Use (kWh/Day) – Avg ± Std	Farm 2 Lighting Energy Use (kWh/Day) – Avg ± Std
1	70.3 ± 5.1	68.9 ± 5.4
2	71.3 ± 2.5	69.3 ± 4.2
3	73.5 ± 2.8	69.0 ± 4.5
4	71.7 ± 4.1	69.5 ± 3.5

Indoor Air Conditions

Histograms of the return air VPD for each farm in each period, with results disaggregated by lighting state, are shown in Figure 13. As mentioned previously, the optimal VPD range for lettuce is roughly 0.8 kPa to 1.0 kPa. The farm temperature and humidity setpoints equate to a VPD of 0.73 kPa for lights on and 0.63 kPa for lights off. Adding a buffer to "ideal" conditions, our analysis considers VPD between 0.6 kPa and 1.2 kPa to be "in range" (Table 7). VPD less than 0.6 kPa reflects conditions that are too humid, while VPD greater than 1.2 kPa indicates conditions that are too dry.

During the baseline monitoring period (Period 1), Farm 1 generally had good indoor conditions, although the farm was sometimes too dry. This is likely explained by a portable dehumidifier placed inside the farm, which the farm operators reported they sometimes used in addition to the monitored

baseline HVAC system in Farm 1, particularly in response to water spills on the floor. The portable dehumidifier use was not monitored, and it was removed for subsequent periods of the study.

In Period 2, the retrofit system (Farm 1) maintained VPD within the target range more often than the baseline Farm 2. However, when conditions in Farm 1 fell outside the target range, they were generally too dry—and in some cases, that dryness was very high (VPD > 1.6 kPa). This finding motivated the design and installation of the bypass to increase the sensible cooling capacity of the retrofit system. In Period 3, following installation of the bypass, conditions in Farm 1 improved substantially, with VPD remaining within the target range 79.5 percent of the time. We attribute this improvement primarily to the bypass, although colder winter weather may also have contributed through higher compressor efficiencies and reduced heat gain from outdoors. In the final evaluation period (Period 4), which included a wider range of outdoor air temperatures, Farm 1 maintained VPD within the target range 73.5 percent of the time with the bypass and improved controls in place.

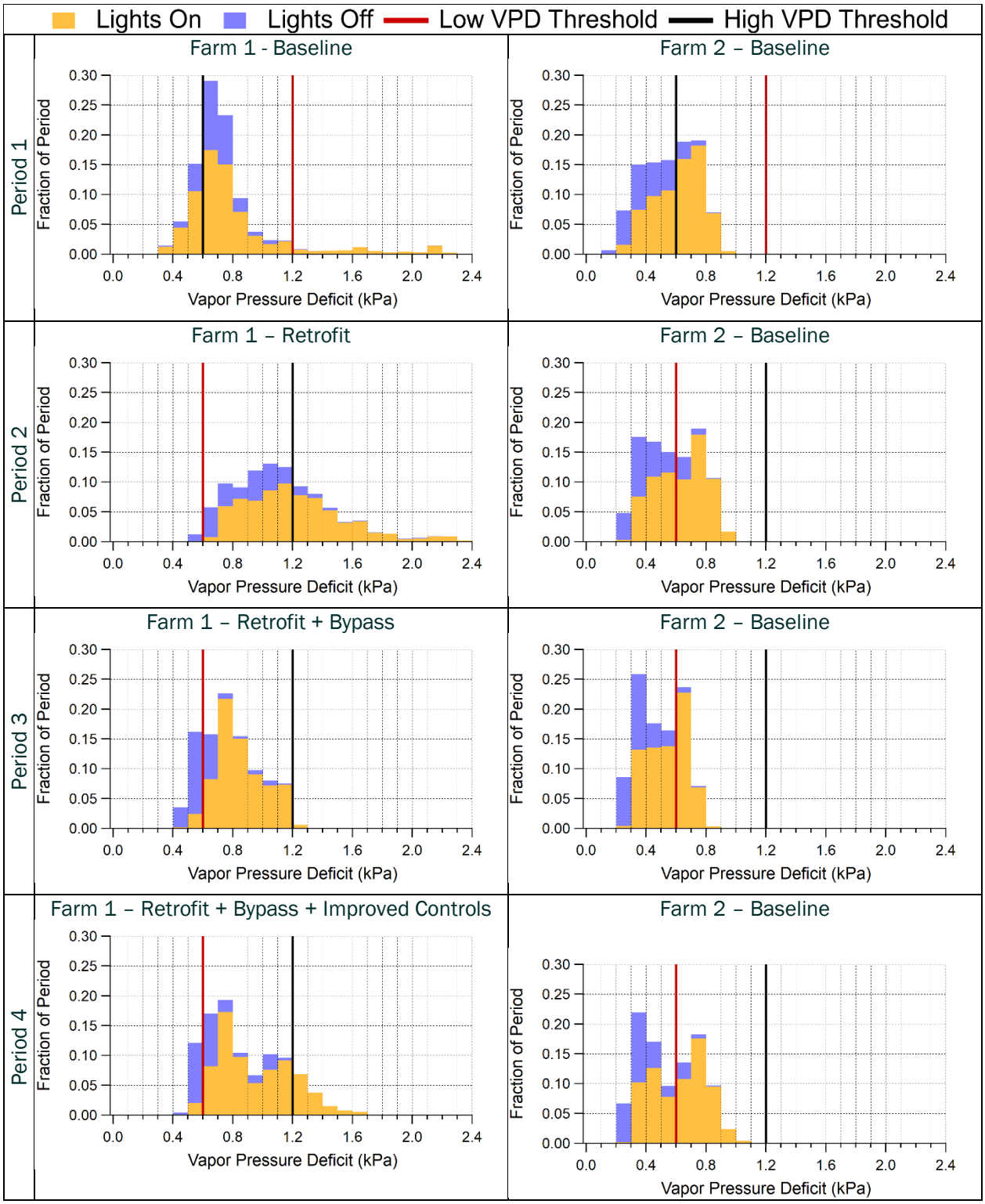

Figure 13: Histograms of each farm's VPD distribution across all periods, disaggregated by lights on/off.

Table 7: Analysis of VPD frequency for each farm across all analysis periods.

Period	Farm 1 Outdoor Air Temp (°F) Avg ± Std	Farm 1 VPD < 0.6 kPa Too Humid	Farm 1 0.6 ≤ VPD ≤ 1.2 In Range	Farm 1 VPD > 1.2 Too Dry	Farm 2 Outdoor Air Temp (°F) Avg ± Std	Farm 2 VPD < 0.6 kPa Too Humid	Farm 2 0.6 ≤ VPD ≤ 1.2 In Range	Farm 2 VPD > 1.2 Too Dry
1	54.7 ± 11.1	22.1	70.3	7.5	56.3 ± 11.2	54.4	45.6	0
2	66.5 ± 10.3	1.3	62.5	36.3	69.3 ± 10.3	54.3	45.7	0
3	50.2 ± 6.3	19.9	79.5	0.6	51.1 ± 6.9	68.7	31.3	0
4	57.5 ± 10.5	12.7	73.5	13.8	58.7 ± 11.1	55.4	44.6	0

Across monitoring periods, the indoor conditions in Farm 2 with the baseline equipment were frequently too humid, with the VPD in the target range less than half the time. In May 2026, we determined that the Farm 2 temperature and humidity sensor used to control the baseline HVAC system was biased low by about 10 percent RH and biased high by about 3°F. The historical data indicates that this offset was present for the duration of the study, which means that the environment was unintentionally controlled to a minimum VPD of 0.44 kPa for lights on and 0.38 kPa for lights off. Reviewing the historical data shows that this issue was not present in Farm 1.

Given that RH offset in Farm 2, comparing the indoor conditions at Farm 1 between Period 1 and Period 4 is especially valuable. VPD remained within the target range for about the same percentage of Period 1 and Period 4 (70.3 percent in Period 1 versus 73.5 percent in Period 4). The retrofit system, when outfitted with the partial heat exchanger bypass and improved control algorithm, performed similarly to the baseline equipment in managing indoor conditions.

Average Daily HVAC Energy Use

To quantify HVAC energy use, the team created bar graphs of average daily HVAC energy use for each farm in each period (Figure 14). The average daily HVAC energy use is the sum of the average daily energy use of each HVAC component (compressor, indoor fan, and heater), disaggregated by lighting status.

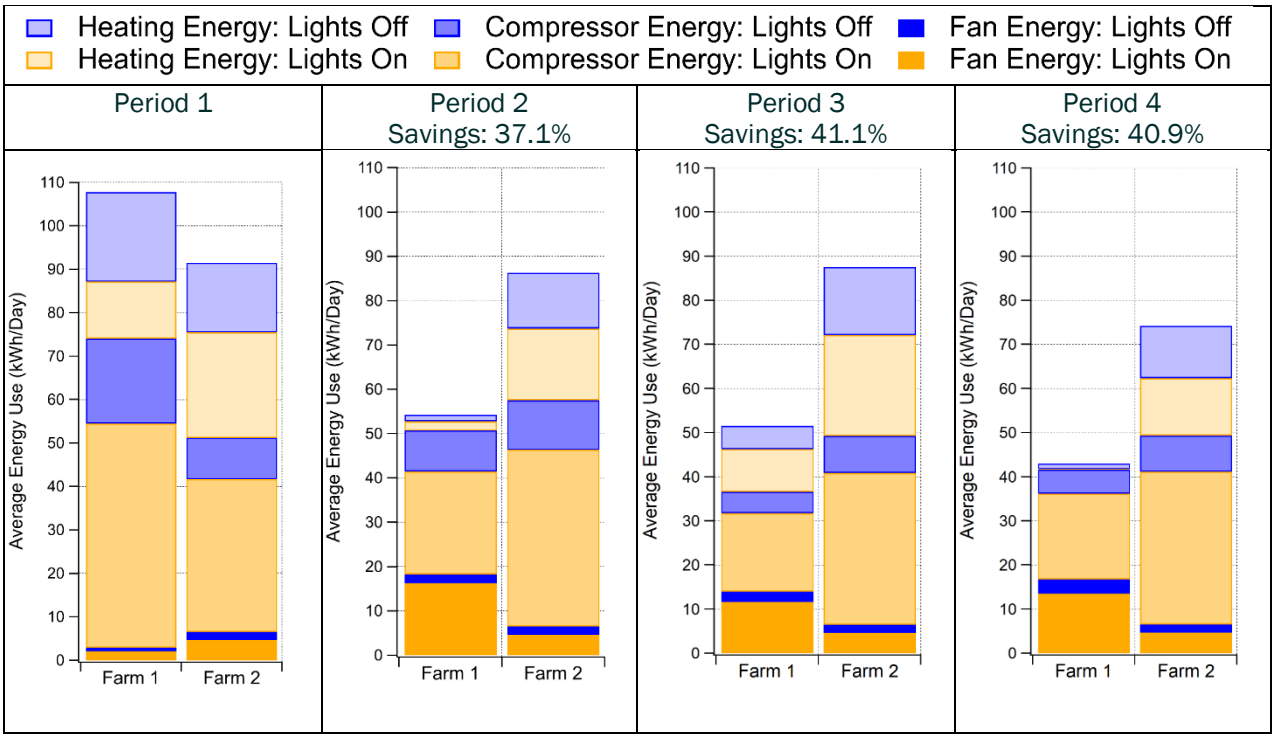

Figure 14: Bar graphs of average daily HVAC energy use for each farm across all analysis periods, disaggregated by HVAC component and lights on/off.

In Period 1, the average daily HVAC energy use was 107.8 kilowatt-hours (kWh) in Farm 1 and 91.5 kWh in Farm 2, a difference of 18 percent. This finding is unexpected, as both farms operated with the same HVAC equipment, comparable loads, and similar weather in this period. Compressor energy use was the leading contributor to this difference—71.1 kWh at Farm 1 versus 44.7 kWh at Farm 2. We attribute this difference primarily to the higher humidity in Farm 2 due to the 10 percent RH offset error in the humidity sensor, as discussed in the Indoor Air Conditions section. The higher humidity in Farm 2 means that the equipment expended less energy for dehumidification. Another contributing factor may be that deciduous trees shade at Farm 2 reduced the solar radiant load during the summer; this was not a factor at Farm 1.

In Period 2, the average daily HVAC energy use was 54.3 kWh in Farm 1 and 86.3 kWh in Farm 2. A Welch's two-sample t-test confirms that the difference in HVAC energy use between the two farms in this period is statistically significant ($p < 0.001$), amounting to an average energy savings of 37.1 percent provided by the retrofit system. These savings came primarily out of reduced reheat energy—the average daily heater energy use was 3.6 kWh in Farm 1 and 28.8 kWh in Farm 2. The retrofit system consumed more fan energy than the baseline HVAC system at Farm 2, as the retrofit system indoor fan draws about 1 kW at high speed and about 0.35 kW at low speed. In contrast, the fan at Farm 2 is fixed speed and consistently draws about 0.275 kW.

In Period 3, the average daily HVAC energy use was 51.6 kWh in Farm 1 and 87.6 kWh in Farm 2, which is an average energy savings of 41.1 percent attributed to the retrofit system. A Welch's two-sample t-test confirms that the difference in HVAC energy use between the two farms in this period is

statistically significant ($p < 0.001$). Again, these savings are attributed primarily to reduced reheat energy use by the retrofit system.

In Period 4, the average daily HVAC energy use was 43.9 kWh in Farm 1 and 74.2 kWh in Farm 2, which equates to an average energy savings of 40.9% attributed to the retrofit system. A Welch's two-sample t-test confirms that the difference in HVAC energy use between the two farms in this period is statistically significant ($p < 0.001$). Although average reheat energy use in both farms decreased from Period 3 to 4 as the weather warmed, it is notable that the average reheat energy consumed by the retrofit system was near 0, which is attributed to the improved controls deployed for Period 4.

Note that in Periods 2 to 4 we cannot disentangle the impact of the humidity sensor offset or shading on the baseline Farm 2 system and therefore do not account for these effects explicitly. However, this limitation implies that, for Periods 2 and 4 where we compare the baseline HVAC to the retrofit HVAC, the energy savings attributed to the retrofit system are likely underestimated. This is because Farm 2 baseline HVAC energy use would be higher if the humidity sensor were correctly calibrated and if the farm had no summer shading. Comparing the HVAC energy use at Farm 1 between Period 1 and Period 4 provides an estimate of what the energy savings may have looked like had these two differences not been present at Farm 2. Farm 1's average HVAC energy use was 107.8 kWh/day in Period 1 and 43.9 kWh/day in Period 4. This amounts to an average energy savings of 59.3% associated with the retrofit system.

Average Daily HVAC Energy Use On-Peak

To quantify any energy savings provided by the retrofit system during peak demand hours, the team graphed the average daily on-peak HVAC energy use for each farm in each period, as shown in Figure 15 below. Peak hours were defined as 16:00 to 21:00. The error bars represent one standard deviation in the average daily on-peak HVAC energy use.

Across all periods, Farm 1 used less HVAC energy during peak hours than Farm 2, although during Period 1—when both systems were operating with baseline HVAC equipment—the difference was small. With the retrofit system, daily energy use during peak hours was reduced by an average of 5.5 kWh/day (29.5 percent) in Period 2, 5.2 kWh/day (29.8 percent) in Period 3, and 3.9 kWh/day (24.8 percent) in Period 4. For each period, we performed Welch's two-sample t-test to determine if the difference between each farm's average daily on-peak HVAC energy use was statistically significant—the tests confirmed they were ($p=0.03$ for Period 1 and $p < 0.001$ for Periods 2 to 4).

Comparing on-peak HVAC energy use at Farm 1 between Period 1 and Period 4, we found that the retrofit system's on-peak energy use was 5.6 kWh/day less than the baseline system in Period 1, amounting to an average on-peak energy savings of 32.3 percent.

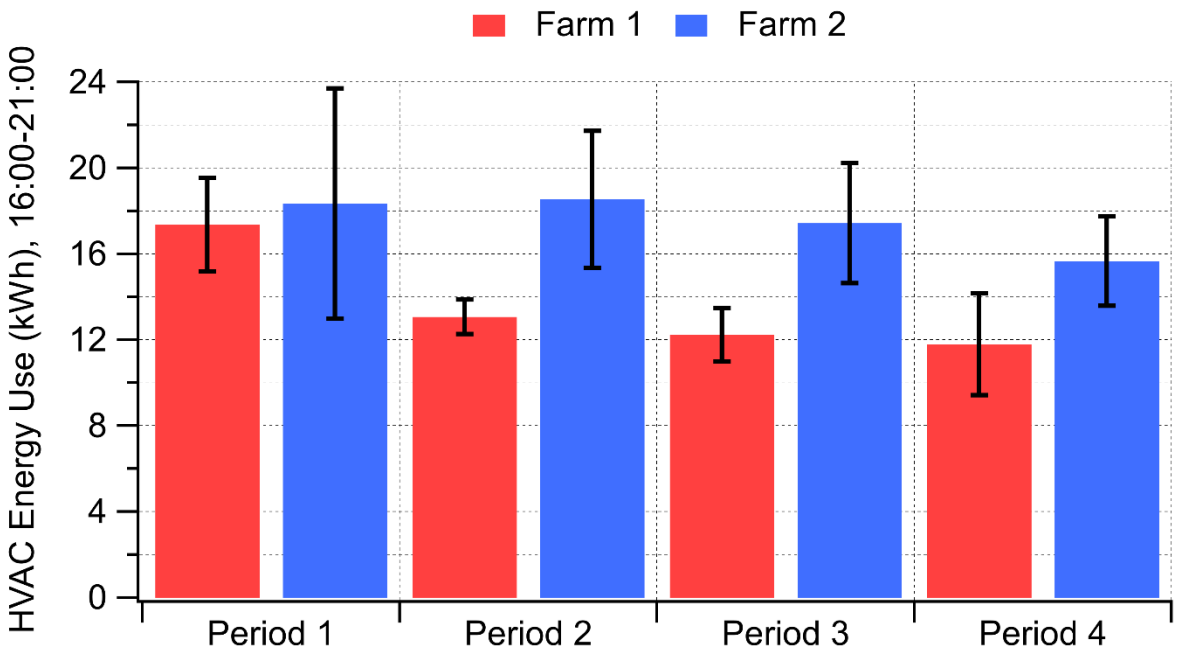

Figure 15: Bar graph depicting the average daily on-peak HVAC energy use at each farm in each period.

Farm 1 HVAC Energy Use: Period 1 Versus Period 4

As noted previously, comparing Farm 1's HVAC energy use in Period 1 (when it was equipped with the baseline HVAC system) to Farm 1's HVAC energy use in Period 4 (when it was equipped with the final retrofit installation) allowed us to evaluate the retrofit system relative to the baseline without the confounding effects of the RH offset error and deciduous tree shading at Farm 2. In Average Daily HVAC Energy Use, we found that the retrofit system in Period 4 used 59.3 percent less energy, on average, than the baseline system in Period 1. To explore Farm 1's HVAC energy use in Periods 1 and 4 further, we plotted each period's daily HVAC energy use against the corresponding daily average outdoor air temperatures (Figure 16) and fit quadratic curves to the data.

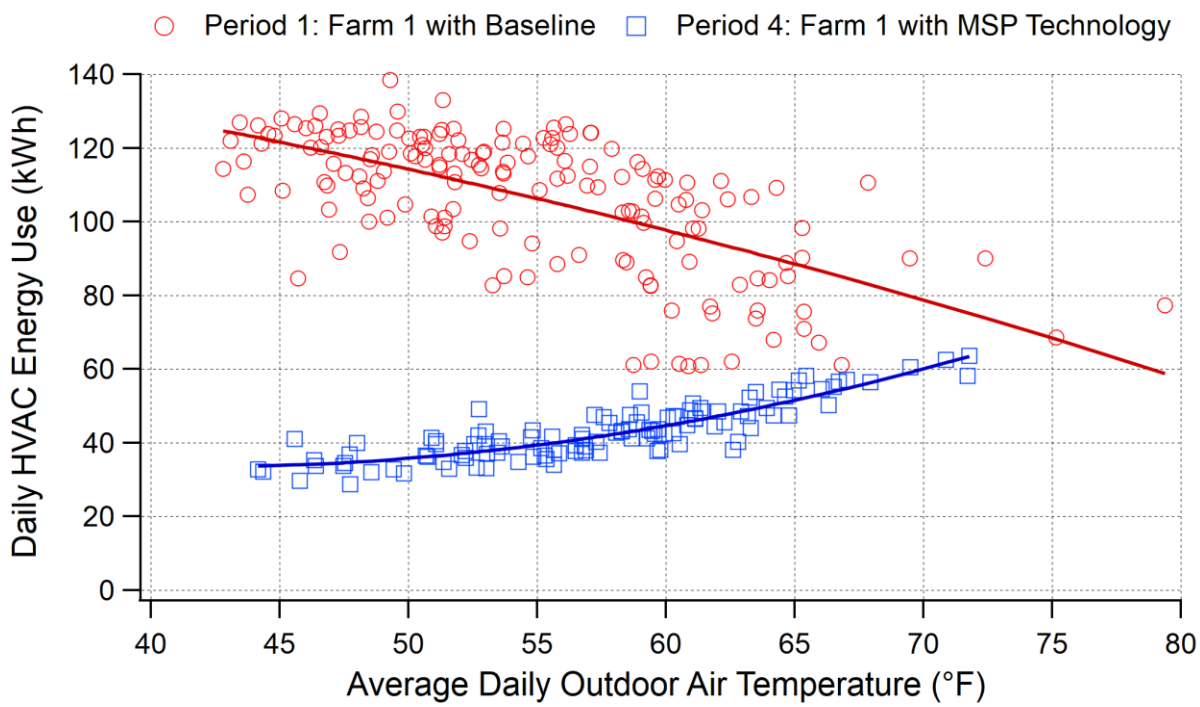

Figure 16: Farm 1's daily HVAC energy use versus average daily outdoor air temperature in Periods 1 and 4.

The best-fit equations and adjusted coefficient of determination (R^2) values, which indicate the quality of fit, are listed in Table 8 below.

Table 8: Best fit equations and adjusted R^2 values.

	Period 1: Farm 1 with Baseline HVAC	Period 4: Farm 1 with Retrofit HVAC
Best Fit Equation	$E = 161.2 - 0.3442 \times OAT - 0.1191 \times OAT^2$	$E = 90.27 - 2.735 \times OAT + 0.03291 \times OAT^2$
Adjusted R^2	0.4009	0.7656

To estimate annual energy savings, the team obtained a TMY weather file from the National Solar Radiation Database for the demonstration site location and applied the best-fit equations developed from the measured data. The TMY file provides hourly outdoor air temperatures for a representative year, so the team calculated the daily average outdoor air temperature for each day of the year and used these values as inputs to the best-fit equations to predict daily HVAC energy use under typical weather conditions. Over the year, the baseline HVAC system was expected to consume 35,342 kWh, and the retrofit system was expected to consume 17,152 kWh—amounting to energy savings of 51.5 percent associated with the retrofit system.

Results: Period 4 with Refined Retrofit HVAC Operation

The following sections analyze HVAC performance and efficiency for Period 4, when the retrofit system had been fully refined.

HVAC Operating Mode

The frequency of runtime in each HVAC mode was expected to depend on outdoor air temperature, as outdoor air temperature impacts HVAC system capacity as well as heat gains or losses through the container's insulated envelope. The bar graphs in Figure 17 show the frequency of total Period 4 runtime that each HVAC system spent in each mode, binned by outdoor air temperature. Note that Farm 1 experienced outdoor air temperatures up to 95°F during this period, while Farm 2 experienced outdoor air temperatures up to 100°F.

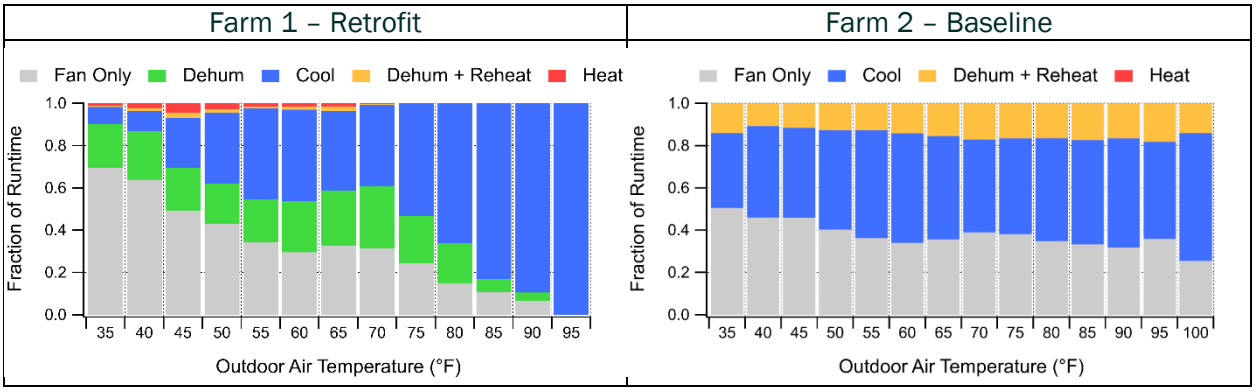

Figure 17: HVAC mode frequency versus outdoor air temperature for Farm 1 and Farm 2 during Period 4.

As Figure 17 shows, HVAC mode frequency was highly dependent on outdoor air temperature at Farm 1. The frequency of Mode 3 (cool) increased with outdoor air temperature, likely due to greater sensible heat gain through the container envelope. Because the retrofit system in Farm 1 rarely overcooled, Mode 4 (dehumidify + reheat) and Mode 5 (heat) were used minimally and only at lower outdoor air temperatures.

In Farm 2, HVAC mode frequency had minimal temperature dependance, with the sum of Mode 2 (cool) and Mode 4 (dehumidify + reheat) appearing to increase slightly as temperature increased. The weaker dependence could be attributed to the deciduous tree shading the container during the summer months, suggesting that solar radiation was a meaningful contributor to heat gain from the outdoor environment.

HVAC Capacity and Efficiency

HVAC performance as a function of outdoor weather conditions is presented below as plots of sensible and latent cooling capacity versus outdoor air temperature, as shown in Figure 18. Data were disaggregated by mode, and we calculated cooling capacity for steady-state operation only, which was defined as at least 5 minutes of compressor operation for dehumidify and dehumidify + reheat modes and at least 10 minutes of compressor operation for cool mode. The scatter in the plots is attributed to a range of return air wet-bulb temperature, which will be discussed further in the Results: Modeling Inputs section.

In cool mode, the sensible and latent capacity for the retrofit system both decreased with increasing outdoor air temperature, as expected. To reiterate, the cool mode runs high fan speed with the bypass open to increase sensible cooling. Since only 20 percent of the air is bypassed, the latent capacity was still generally higher than the sensible capacity, and the average SHR for cool mode operation was 0.39.

In cool mode, the sensible capacity for the baseline HVAC also decreased with outdoor air temperature, although less drastically than was observed for the retrofit system. The baseline HVAC latent capacity remained approximately constant across outdoor air temperatures. The sensible capacity was consistently higher than the latent capacity for the baseline HVAC (which had an average SHR of 0.66), which was expected for a conventional air conditioning system. The sensible capacity for the baseline HVAC was higher than for the retrofit system, especially at high outdoor air temperatures, which is a benefit when lettuce plants are small and minimally transpiring (i.e., converting sensible heat to latent heat).

In dehumidify mode, the sensible and latent capacity for the retrofit system also decreased with increasing outdoor air temperature, with latent capacity decreasing more drastically. As previously mentioned, the dehumidify mode closes the bypass and operates the fan at low speed to minimize sensible cooling and maximize dehumidification; this led to minimal sensible cooling and an average SHR of 0.15, as intended. The baseline HVAC system at Farm 2 does not have a comparable dehumidify mode—the high dehumidification capacity achieved with the retrofit system is the major strength of the equipment.

In dehumidify + reheat mode, the sensible and latent capacity for the retrofit system remained approximately constant with increasing outdoor air temperature. There are limited data in this mode, as the heat recovery heat exchanger drastically limits the need for electric reheat. As expected, the sensible capacity was negative, meaning that the air temperature of the supply air was warmer than the return air (i.e., it was heated).

In dehumidify + reheat mode, the sensible and latent capacity for the baseline HVAC also remained approximately constant with increasing outdoor air temperature. Data in this mode was plentiful, since it was the only dehumidification mode for the baseline HVAC. As the team anticipated, the sensible capacity was negative, meaning that the air temperature of the supply air was warmer than the return air (i.e., it was heated).

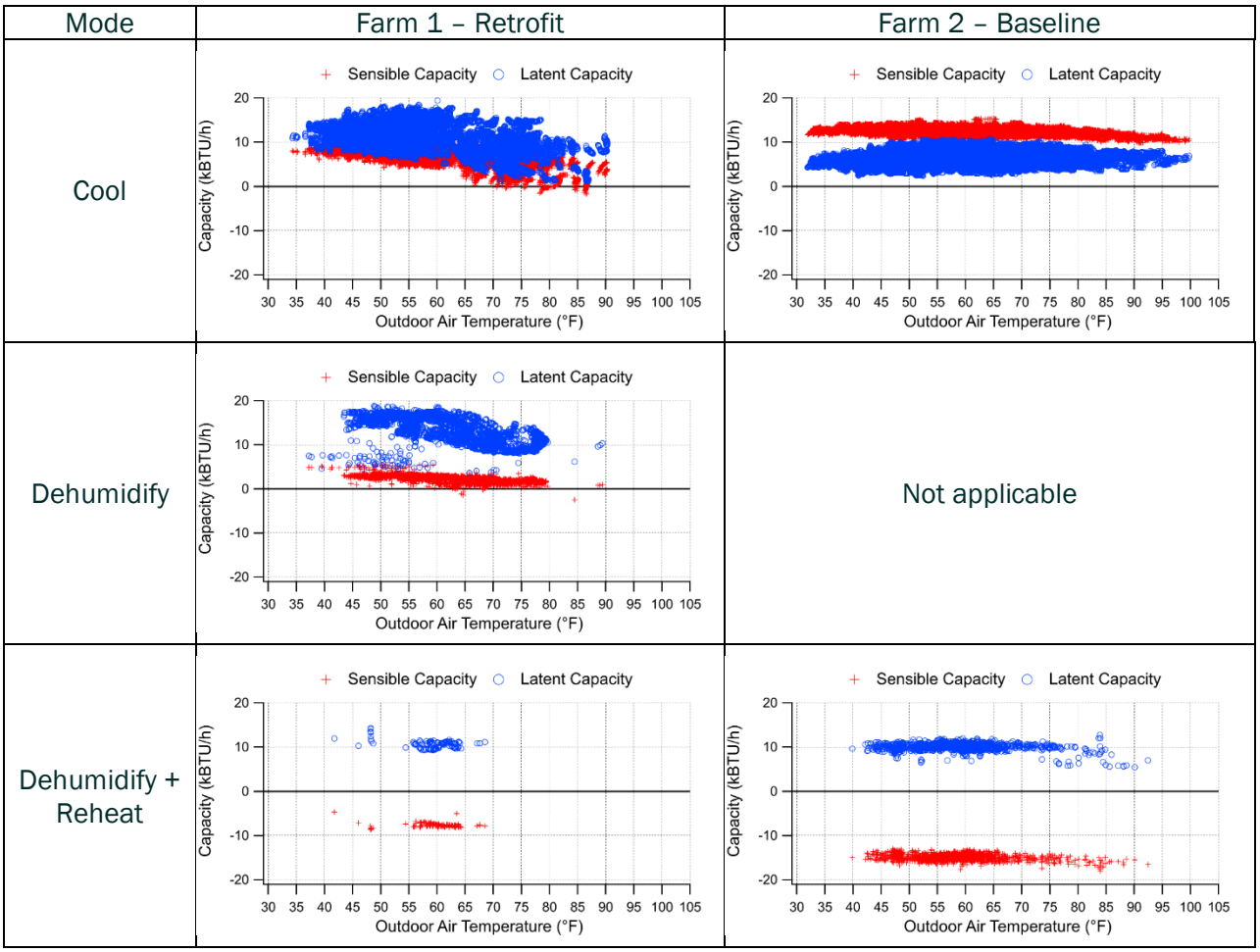

Figure 18: Plots of latent capacity and sensible capacity for three cooling and dehumidification modes in both farms.

HVAC efficiency as a function of outdoor weather conditions is presented below in Figure 19 as plots of COP versus outdoor air temperature for each HVAC mode at each farm. We calculated the COP for steady-state operation by dividing the total capacity data (sensible plus latent) presented in Figure 18 with the coincident power data.

Mode	Farm 1 – Retrofit	Farm 2 – Baseline
Cool	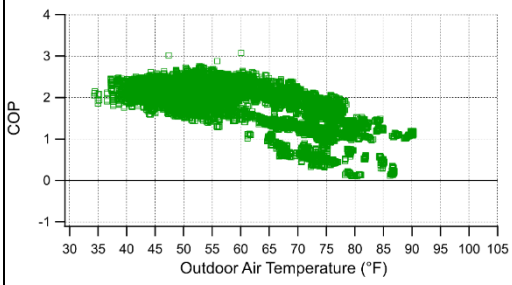	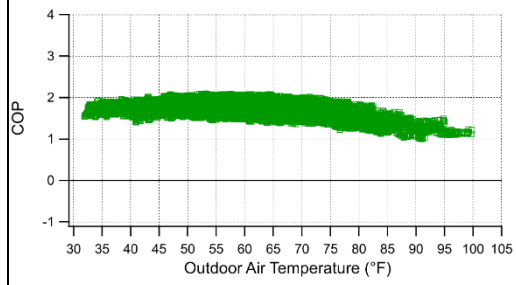
Dehumidify	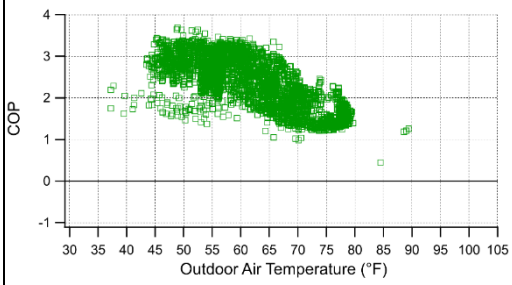	Not applicable
Dehumidify + Reheat	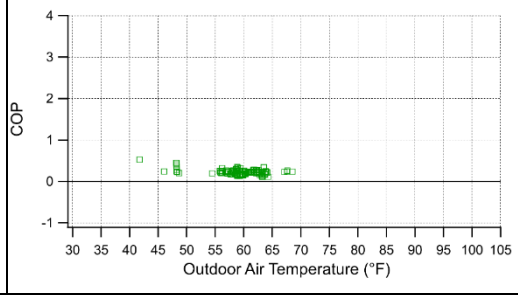	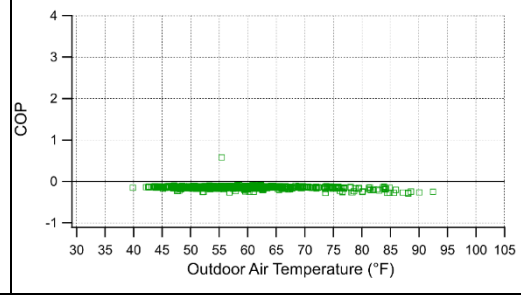

Figure 19: Plots of total COP for three cooling and dehumidification modes in both farms.

In cool mode, the COP for the retrofit system was relatively constant at outdoor air temperatures less than 65°F. This may be attributed to the single-speed compressor design with low ambient controls that modulate the condenser fan to maintain a liquid line temperature of 70°F—achieving higher efficiency at lower outdoor air temperatures would require employing a variable speed compressor. Above 65°F, COP decreased with increasing outdoor air temperature. There was considerable variance in the COP data, especially at higher outdoor air temperatures; this likely occurred during times when the indoor conditions in the farm were drier, which happens when lettuce plants are small and minimally transpiring.

In cool mode, the COP for the baseline HVAC remained similarly constant at outdoor air temperatures less than 70°F and then decreased, suggesting that the baseline HVAC with a single-speed compressor uses similar low-ambient controls. The baseline HVAC COP had less variance and was higher than the retrofit system COP at high outdoor air temperatures, likely due to the higher sensible cooling capacity and thus, the higher indoor wet-bulb temperatures observed.

In dehumidify mode, the retrofit system's COP decreased with increasing outdoor air temperatures, with a maximum of approximately 3 at 50°F. This mode was expected to achieve the highest COP of

all operating modes, as it best reflects the retrofit system's design conditions and intended use. The baseline HVAC system does not have a comparable mode.

In dehumidify + reheat mode, the COP remained constant with increasing outdoor air temperature for both HVAC systems. The COP was close to zero in this mode for both farms because the electric heater operation increases the total HVAC power draw and decreases the total capacity. For the baseline HVAC, the COP was negative, indicating that the sensible heat added by the electric heater was greater than the latent heat removed by the cooling coil.

In the previous laboratory testing of the retrofit system (Ross, McMurry and Pistochini 2016), capacity and COP were measured for a range of indoor dry-bulb temperatures, indoor wet-bulb temperatures, outdoor dry-bulb temperatures, and airflow rates. To compare the real-world performance of the retrofit system to the laboratory test results, we sought to match field data to laboratory test conditions and compare the corresponding capacities and COP. However, in the laboratory testing, the retrofit system was not equipped with a bypass or electric resistance heater. We therefore limited our analysis to a comparison of the dehumidify mode field data to three laboratory tests conducted with an airflow rate of 900 CFM (compared to field airflow rate of 830 CFM); an indoor dry-bulb temperature of 75°F; an indoor wet-bulb temperature of 62.4°F; and outdoor air temperatures of 55°F, 75°F, and 95°F. The sensible capacity, latent capacity, and COP as a function of outdoor air temperature are plotted in Figure 20 below for both the field data and the laboratory tests.

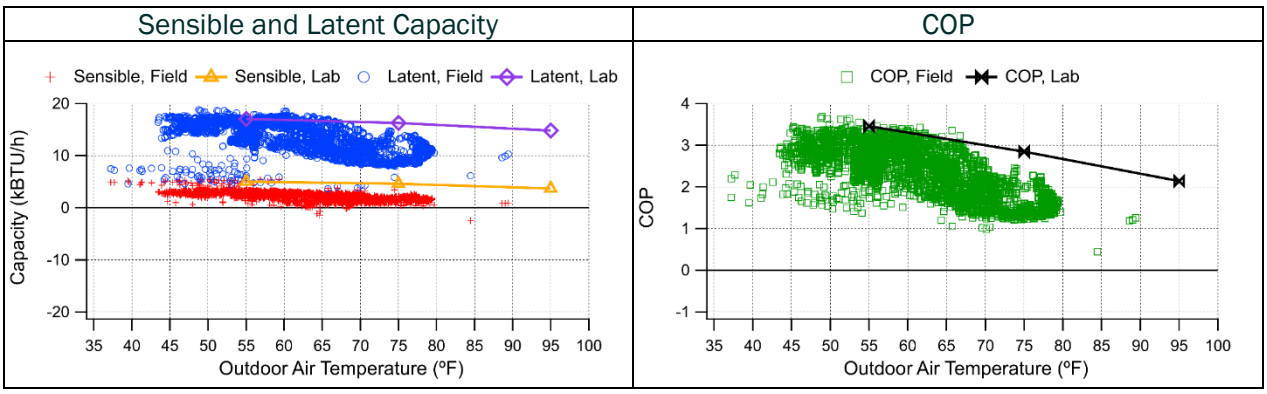

Figure 20: Plots of field and laboratory sensible and latent capacity (left) and COP (right) for the retrofit system in dehumidify mode.

Generally, the laboratory results were higher than the field results at all three outdoor air temperatures. The laboratory tests were all conducted at higher indoor dry-bulb and wet-bulb temperatures than the farms typically operated at. For comparison, the average indoor dry-bulb temperature for the field data presented in Figure 20 was 64.3°F, and the average indoor wet-bulb temperature was 57.6°F—both of which are meaningfully lower than the laboratory test conditions. Since capacity and COP decrease with decreasing return dry- and wet-bulb temperatures, this likely explains the differences between the laboratory and field data. Additionally, differences in test methodology may contribute to the observed discrepancies between laboratory and field performance: laboratory test procedures measured steady-state performance over a one-hour test period, whereas the field data apply a five-minute steady-state threshold, reflecting the fact that long continuous operating periods are not typically observed in real field conditions. As a result, this

approach may still capture the effects of transient cycling behavior, which generally reduces capacity and efficiency.

Results: Modeling Inputs

An important outcome of field studies is the ability to synthesize the results into modeling inputs that can be used to predict energy savings across different climates and outdoor weather conditions. The team derived three key modeling inputs from this study:

1. Sensible heat generation from the grow lights and external heat flux through the insulated container walls
2. Moisture generation rates, which determine the conversion of sensible heat to latent heat loads
3. Equipment performance curves for both the baseline HVAC system and the retrofit system

Sensible Load Generation Rate: Lighting and External Heat Flux

Understanding the sensible heat load on the container farm is important for development of an energy balance model of the farm. All energy added to the farm initially enters as sensible heat from the lighting system and heat flux through the farm's insulated envelope. A portion of this sensible heat is subsequently converted to latent heat through plant transpiration and other evaporation processes. We quantified the sensible heat load from the lights through power metering; the heat gain from the grow lights was 6.1 kBTU/h for blue lights only, 11.3 kBTU/h for red lights only, and 17.4 kBTU/h for simultaneous red and blue operation.

As discussed earlier in this report, we hypothesized that Farm 1 experienced higher external heat gains than Farm 2 due to shading from deciduous trees at Farm 2. This external heat gain was also expected to increase with outdoor air temperature. To quantify external heat flux for model development of container farms, we assumed that grow lights represent the only internal heat source within the farms. Under this assumption, the team calculated the net external heat flux as the difference between the total heat removed by the HVAC system and the total heat added by the grow lights over each time interval.

Specifically, for each hour in Period 4, we computed the hourly external heat flux by subtracting the summed grow light heat input from the summed HVAC heat removal. This calculation assumes the HVAC system maintains setpoint conditions and therefore removes all internal and external heat gains; accordingly, data were filtered to include only hours in which the hourly average return air temperature was below the temperature setpoint. Figure 21 presents the resulting relationship between hourly external heat flux and average outdoor air temperature.

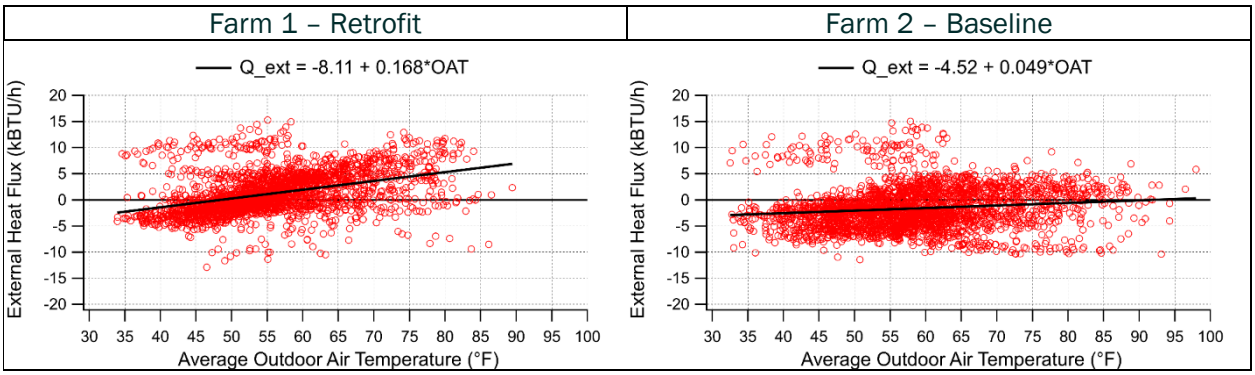

Figure 21: Plots of hourly external heat flux versus hourly average outdoor air temperature for Farm 1 (left) and Farm 2 (right).

As these plots show, the external heat flux generally increased with outdoor air temperature at both farms, as expected. However, the external heat flux increased more dramatically with outdoor air temperature at Farm 1 than at Farm 2. We calculated a line of best fit for the external heat flux as a function of outdoor air temperature, and the slope of Farm 1's best fit line is more than three times larger than the slope of Farm 2's best fit line. This finding is consistent with the theory that the shading of Farm 2 reduces the total load on the HVAC system.

This difference becomes non-trivial at high outdoor air temperatures. For example, at 85 °F, the predicted external heat flux is 6.2 kBTU/h for Farm 1 and negligible for Farm 2; the additional environmental heat gain in Farm 1 therefore represents a non-negligible fraction of the total heat gain. This added load partially explains why the retrofit system struggled to provide sufficient sensible cooling at high outdoor air temperatures, particularly during periods when both red and blue lights are operating during peak daytime conditions.

In the simple indoor farm model developed by Ross, McMurry, and Pistochini, sensible heat load was assumed to arise solely from lighting, with an assumed lighting power density of 30 watts per square foot (W/ft^2) (Ross, McMurry and Pistochini 2016). This value was higher than the peak lighting power density observed at the field site (17 W/ft^2), which is likely more representative of container farms that grow lettuce. However, other crops may require higher lighting power densities, as the lights in the container farms employed in this study were not configured to operate at maximum output.

Moisture Generation Rate

To quantify the moisture generation rate for model development of container farms, we analyzed the latent load produced by crop irrigation and plant transpiration. This latent load represents a phase change process in which sensible heat is converted into latent heat through evaporation. As a result, an equivalent amount of sensible heat is removed from the system as is added in latent form.

The moisture generation rate is expected to be higher when the grow lights are on, since photosynthetic activity increases plant transpiration. Accordingly, the moisture generation rate was estimated separately for lights-on and lights-off conditions. To estimate the moisture generation rate, we calculated the total moisture removed by each HVAC system for each day in Period 4, disaggregated by lighting status, and divided by the number of hours of runtime (Figure 22).

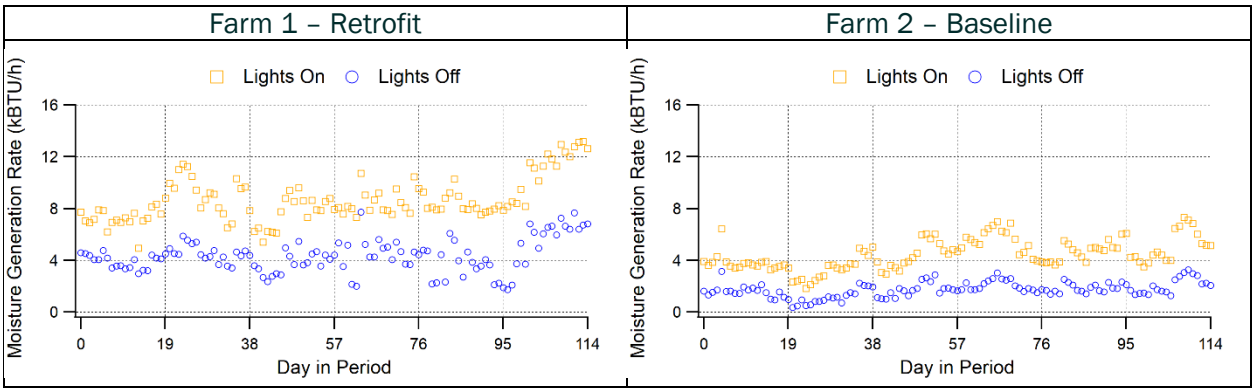

Figure 22: Average daily moisture generation rates for Farm 1 (left) and Farm 2 (right) in Period 4.

With lights on, the average moisture removal rate was 8.7 kBTU/h in Farm 1 (retrofit HVAC) and 4.5 kBTU/h (baseline HVAC) in Farm 2. With lights off, the average moisture removal rate was 4.3 kBTU/h in Farm 1 and 1.7 kBTU/h in Farm 2. Since Farm 2 was more humid than the design conditions (see Indoor Air Conditions), the average observed moisture removal rate is likely to underestimate the moisture generation rate that would occur in ideal conditions. In Farm 1, where the conditions were generally within the ideal range, the average moisture removal rate is likely a good approximation of the moisture generation rate for a model container farm.

In the simple indoor farm model developed by Ross, McMurry, and Pistochini, the moisture generation rate was assumed to be 0.25 gallons per day per square foot (gpd/ ft²) to 2 gpd/ ft² (Ross, McMurry and Pistochini 2016). Using a latent heat of vaporization for water of 8.7 kBTU per gallon, the average results derived from Figure 22 correspond to 20.9 gallons per day for Farm 1, or approximately 0.1 gpd/ ft². when normalized over the 220-square-foot growing area. The value observed in this field study is likely a better estimate for modeling actual container farms that grow lettuce than the prior model assumptions. However, transpiration rates are expected to vary depending on crop type and growing conditions.

Equipment Performance Curves

The data contained in Figure 18 and Figure 19 were used to build equipment cooling performance curves for modeling purposes. The method for modeling cooling equipment performance is generally to fit available data to a series of best-fit biquadratic performance curves. For an air-cooled condenser and indoor cooling coil, total cooling capacity ($Q_{Cooling,\ Total}$) and power (P) are a function of outdoor dry-bulb temperature ($T_{db,out}$) and indoor wet-bulb temperature ($T_{wb,in}$), per Equation 13 and Equation 14:

$$Q_{Cooling,\ \dot{T}otal} = a + b \times T_{wb,in} + c \times {T_{wb,in}}^2 + d \times T_{db,out} + e \times {T_{db,out}}^2 + f \times T_{wb,in} \times T_{db,out}$$

Equation 13

$$P = a + b \times T_{wb,in} + c \times {T_{wb,in}}^2 + d \times T_{db,out} + e \times {T_{db,out}}^2 + f \times T_{wb,in} \times T_{db,out}$$

Equation 14

For an air-cooled condenser and indoor cooling coil, the SHR is a function of indoor dry-bulb temperature ($T_{db,in}$) and indoor wet-bulb temperature ($T_{wb,in}$), per Equation 15:

$$SHR = a + b \times T_{wb,in} + c \times T_{wb,in}{}^2 + d \times T_{db,\text{in}} + e \times T_{db,in}{}^2 + f \times T_{wb,in} \times T_{db,\text{in}} \quad [15]$$

Equation 15

While the retrofit system also includes a plate heat exchanger for heat recovery, we applied the modeling framework described in Equation 13 through Equation 15 and evaluated the resulting model fit. Best-fit curves and the corresponding input data are shown in figures provided in the Appendix, and the resulting coefficients and curve-fitting statistics are summarized in Table 9 for cool mode and Table 10 for dehumidify mode. The result for power includes the compressor, indoor fan, condenser fan, and all ancillary electronics. Note that predictions outside the domain of the fitted data, shown in Table 11, represent extrapolations, and the model is expected to perform best under interpolation. Caution is warranted at low outdoor air temperatures due to the quadratic form of the fitted curves, which predicts decreasing performance below approximately 50°F and may lead to large errors outside the input data range.

Table 9: Best-fit equipment performance curve coefficients for the retrofit system in cool mode.

Coefficient	Total Capacity (kBTU/h)	SHR (-)	Power Draw (kW)
a	-2.220E+02	-5.161E+00	5.173E+00
b	8.650E+00	2.261E-01	-9.331E-02
c	-8.271E-02	-1.580E-03	1.269E-03
d	-9.416E-01	-1.556E-02	8.107E-04
e	-8.715E-03	1.024E-03	4.670E-04
f	3.089E-02	-1.508E-03	-8.547E-04
Adjusted R^2	0.86	0.72	0.46
Residual Standard Error	1.35	0.09	0.12

Table 10: Best-fit equipment performance curve coefficients for the retrofit system in dehumidify mode.

Coefficient	Total Capacity (kBTU/h)	SHR (-)	Power Draw (kW)
a	-1.081E+02	Not applicable Average = 0.15 Standard deviation = 0.02	1.481E+00
b	2.823E+00		5.388E-02
c	-1.701E-02		-2.413E-04
d	8.932E-01		-4.739E-02
e	-8.170E-03		6.409E-04
f	-1.435E-03		-3.848E-04
Adjusted R^2	0.88		0.44
Residual Standard Error	1.07		0.12

Table 11: Domain for input data for best-fit equipment curves for the retrofit system.

Mode	Outdoor Dry Bulb Minimum (°F)	Outdoor Dry Bulb Maximum (°F)	Indoor Wet Bulb Minimum (°F)	Indoor Wet Bulb Maximum (°F)	Indoor Dry Bulb Minimum (°F)	Indoor Dry Bulb Maximum (°F)
Cool	34.3	90.3	50.5	62.0	60.3	74.1
Dehumidify	43.5	89.4	51.3	62.3	57.3	71.6

Note that while the domain for the outdoor dry-bulb temperature for the dehumidify mode extends to 90.3°F, there are only three data points above 80°F. Therefore, caution is warranted when using this mode's performance curves above 80°F.

The modeled results for the retrofit system's total capacity showed good agreement for both cool and dehumidify models, with high R^2 values indicating that variation in capacity was well explained by the variables included in the regressions. The residual standard error (RSE) was also reasonable (~1 kBTU/h), representing the typical magnitude of prediction error for the fitted curves. For SHR in cool mode, the model similarly showed a high R^2 value and low RSE. In dehumidify mode, however, we observed minimal correlation between the input variables and resulting SHR—likely because all air passed through the plate heat exchanger in this mode, resulting in relatively low and constant SHR behavior. Therefore, an average SHR value of 0.15 was used for this mode. The R^2 values for

the power models were lower, likely because power draw remained relatively constant below 60°F outdoor temperature. However, the RSE remained relatively low (0.12 kW), indicating that the model still provided a reasonable prediction of power consumption.

Similarly for the baseline HVAC, best-fit curves and the corresponding input data are shown in figures provided in the Appendix, and the resulting coefficients and curve-fitting statistics are summarized in Table 12. The result for power includes the compressor, indoor fan, condenser fan, and all ancillary electronics. Note that predictions outside the domain of the fitted data, shown in Table 13, represent extrapolations, and the model is expected to perform best under interpolation. In particular, caution is warranted at low outdoor air temperatures due to the quadratic form of the fitted curves, which predicts decreasing performance below approximately 50°F and may lead to large errors outside the input data range.

The modeled results for baseline HVAC for all outputs (total capacity, SHR, and power) were excellent, with high R^2 (greater than 0.85) and low RSE values. RSE was 0.4 kBTU/h for capacity, 0.01 for SHR, and 0.07 kW for power.

Table 12: Best-fit equipment performance curve coefficients for baseline HVAC in cool mode.

Coefficient	Total Capacity (kBTU/h)	SHR (-)	Power Draw (kW)
a	1.779E+00	1.980E+00	4.307E-02
b	7.913E-02	-1.271E-01	1.488E-01
c	2.665E-03	-7.075E-04	-1.257E-03
d	-2.179E-02	8.066E-02	-5.939E-02
e	-1.075E-03	-1.311E-03	5.736E-04
f	2.406E-03	2.313E-03	3.859E-05
Adjusted R^2	0.87	0.97	0.88
Residual Standard Error	0.44	0.01	0.07

Table 13: Domain for input data for best-fit equipment curves for baseline HVAC.

Mode	Outdoor Dry Bulb Minimum (°F)	Outdoor Dry Bulb Maximum (°F)	Indoor Wet Bulb Minimum (°F)	Indoor Wet Bulb Maximum (°F)	Indoor Dry Bulb Minimum (°F)	Indoor Dry Bulb Maximum (°F)
Cool	31.9	99.8	50.9	63.8	59.4	70.5

In the section HVAC Capacity and Efficiency, the team compared the field data to previous laboratory testing results for the retrofit system in dehumidify mode (Ross, McMurry and Pistochini 2016). Note that the laboratory tests were conducted with an airflow rate of 900 CFM, compared to field airflow rate of 830 CFM. Here we use the model from Table 10 to calculate the expected results for the laboratory test conditions at 55°F and 75°F outdoor air temperature—which are within the domain of the field data for dehumidify mode—and compared the predicted results to the actual results from the laboratory (Table 14). The field data and resulting model predicts lower capacity, particularly for sensible capacity, and as a result, lower COP than measured in the laboratory testing. As discussed previously, the difference may be attributed to differences in airflow rate, as well as dynamic effects associated with equipment cycling. Another contributor to reduced capacity may be heat gain from solar radiation on the retrofit system's cabinet in the field, which is not present in the laboratory test.

Table 14: Comparison of predicted results derived from a model created from field data to laboratory test results.

	$T_{db, in}$ = 75°F, $T_{wb, in}$ = 62.4°F, $T_{db, out}$ = 55°F		$T_{db, in}$ = 75°F, $T_{wb, in}$ = 62.4°F, $T_{db, out}$ = 75°F	
	Lab Result	Performance Curve	Lab Result	Performance Curve
Sensible Capacity (kBTU/h)	5.04	3.20	4.61	2.42
Latent Capacity (kBTU/h)	17.05	18.11	16.27	13.72
Power	1.87	1.91	2.14	2.15
COP	3.46	3.26	2.85	2.20

Data Analysis

Load Management

A primary objective of this study was to assess the retrofit system's performance in managing the cooling loads in an indoor farm. The team achieved this objective by assessing (and improving) the

retrofit system's ability to manage the indoor farm loads over a nine-month period. In Period 2, the system provided excessive latent cooling and insufficient sensible cooling when outdoor air temperatures were high, as well as when lettuce plants were young with lower transpiration rates.

To partially address this problem, we designed and field-installed a partial bypass of the plate heat exchanger that is open during cool mode, which increased the SHR from an average of 0.15 to 0.39. An additional benefit of the bypass is reduced fan power when the bypass is in use, due to reduced resistance. With the bypass installed (Periods 3 and 4), the retrofit system could provide additional sensible cooling when needed, keeping VPD within the optimal range for most of the runtime (79.5 percent and 73.5 percent, respectively). However, the system still occasionally over-dehumidified during high sensible load conditions. A manufacturer-integrated bypass of the plate heat exchanger that allows a greater fraction of air to bypass the exchanger and achieve a higher SHR (e.g., 0.6) would be expected to further improve performance. An alternative to a plate heat exchanger bypass is installing an additional trim cooling coil at the outlet of the plate heat exchanger. However, this increases equipment cost due to the added coil and does not provide the fan power savings achieved by bypassing the plate heat exchanger.

Energy Savings

Another primary objective of this study was to characterize the energy savings associated with the retrofit system installed at an indoor farm. We achieved this objective, as our data from nine months of monitoring show that the retrofit system provided 37 percent to 41 percent average energy savings relative to the baseline within the same monitoring period, with 25 percent to 30 percent energy savings during peak hours. As expected, most of the energy savings are attributed to less reheat energy use by the retrofit system. The farm operating with the baseline HVAC was unintentionally controlled to a higher indoor relative humidity (~80 percent instead of 70 percent) and benefited from shading from deciduous trees in the summer. This limitation implies that, for Periods 2 and 4, where we compare the baseline HVAC to the retrofit HVAC, the energy savings attributed to the retrofit system are likely underestimated. This is because baseline HVAC energy use would be higher if the humidity sensor were correctly calibrated and if the farm had no summer shading. Indeed, when comparing the retrofit system in Period 4 to the baseline system at Farm 1 in Period 1, which did not experience a sensor offset issue or tree shading, we estimated that the retrofit system provided an annual energy savings of 51.5 percent.

Comparison to Prior Laboratory Study and Model

The final primary objective of this field study was to compare results to prior laboratory testing and modeling of the retrofit system (Ross, McMurry and Pistochini 2016). This was challenging because the laboratory testing was conducted at higher dry-bulb and wet-bulb temperatures. However, using best-fit curves derived from the field data to predict performance at the laboratory test points showed that the field results had similar power consumption but lower cooling capacity in dehumidify mode. Possible reasons for this discrepancy include a lower airflow rate during the field test, dynamic cycling conditions that occur in the field, and solar radiation on the retrofit system's cabinet that was not present during laboratory testing. Even though the field results showed lower efficiency than the laboratory results, the energy savings were still substantial compared to the baseline HVAC technology.

The data obtained from the field study also showed that several assumptions used in the laboratory-developed model were not representative of actual field conditions. The lighting power density in the field was lower than modeled (17 W/ft^2 versus 30 W/ft^2), as were the moisture generation rates (0.1 gpd/ ft^2 versus 0.25 gpd/ ft^2). Additionally, heat gains through the insulated container envelope reached up to 10 kBtu/h at high outdoor air temperatures, demonstrating that the prior modeling assumption of no heat transfer through the envelope was not defensible.

Stakeholder Feedback

Stakeholder engagement primarily consisted of collecting feedback from and sharing results with the farm operators and the manufacturer and distributor of the retrofit system. The team has frequently communicated with the farm operators since the beginning of the study, and their feedback during the initial retrofit process was particularly insightful. For example, the operators emphasized the importance of keeping openings in the farm envelope covered during the retrofit process to avoid introducing pests into the farm. Perhaps the most important takeaway we learned from the farm operators was that maintaining the indoor temperature and relative humidity at target levels was just as important—if not more so—as achieving large energy savings. This feedback further motivated the partial heat exchanger air bypass that improved indoor conditions. Although the indoor conditions are still drier than ideal at times, the operators report no concerns with the growing conditions of the farm.

Our conversations with the manufacturer and distributor of the retrofit system have focused on the retrofit process, observed shortcomings of the system, and potential improvements that could be integrated into future products. We worked with an engineer employed by the manufacturer to design and field install the partial heat exchanger air bypass, and the manufacturer appears open to the possibility of integrating a bypass design into the packaged geometry of the unit.

In February 2026, the team had a poster and presented project results at the ASHRAE Winter Conference (Figure 23). At the conference, we also met with the manufacturer's same engineer and the sales manager to talk about the project and present performance results. During that conversation, we discussed how the retrofit system is typically deployed in larger buildings with a chilled water coil and chiller instead of refrigerant coil with condensing unit. In these larger systems, customers generally specify a secondary cooling coil fed by chilled water for SHR control. This project has been valuable in assessing product performance for the smaller, lower-cost system built for the container farm application.

Figure 23: Presentation at ASHRAE 2026 Winter Conference.

The team has also developed a relationship with the manufacturer of the container farms. We informed them of the project at the beginning of the study and provided them with updates as the study progressed. They are enthusiastic about the observed energy savings. An engineer with the manufacturer helped us program and implement the new control algorithm for the retrofit system on the farm's backend. This relationship has been very important for technology transfer, as we have made the manufacturer aware of alternative HVAC solutions for indoor farming.

On May 20, 2026, the team met with representatives from the manufacturer of the retrofit HVAC system, the equipment distributor, and the container farm manufacturer to present results from the study and discuss next steps. All parties were excited by the energy savings achieved in the study, and the container farm manufacturer also expressed interest in further research exploring the performance of the retrofit system relative to other HVAC technologies for indoor farming.

Recommendations

This study has shown that the retrofit system can provide substantial energy savings for indoor farms but may over dehumidify and not meet temperature setpoints when sensible heat loads are high. Indoor farmers looking to reduce their energy consumption could benefit from this system, as long as they integrate means to modulate the SHR of the system through a secondary cooling coil or a partial heat exchanger bypass.

Limitations

The baseline HVAC was unintentionally controlled to a higher indoor relative humidity (~80 percent instead of 70 percent) and benefited from shading from deciduous trees in the summer. This limitation implies that, for Periods 2 and 4, where we compare the baseline HVAC to the retrofit HVAC, the energy savings attributed to the retrofit system using this approach are likely

underestimated. This is because baseline HVAC energy use would be higher if the humidity sensor was correctly calibrated and if the farm had no summer shading. Our comparison of Farm 1 during Periods 1 and 4, before and after the HVAC retrofit, estimated energy savings of 51.5 percent for a typical weather year.

Future Research

Future research efforts could use the available study data to predict outcomes for the retrofit system across California climate zones, potentially for a range of related applications—e.g., other crops with different indoor environment conditions, lighting requirements, and moisture generation rates. This future research could also evaluate another HVAC system design that uses condenser heat recovery for reheat (as opposed to electric reheat), which is expected to be more efficient than the baseline HVAC system tested here but less efficient than the retrofit system. Additional future studies on other potential applications of the retrofit system are possible, such as industrial dehumidification applications and commercial buildings with high dehumidification loads, like indoor swimming pools.

References

n.d. *CalNEXT.* Accessed 10 18, 2023. https://calnext.com/.

Ross, Derrick, Robert McMurry, and Theresa Pistochini. 2016. *Laboratory Testing of MSP Technology's Dehumidification System.* Final Project Report, Davis: UC Davis Western Cooling Efficiency Center.

Sabeh, Nadia. 2020. *VPD: The Pressure to Transpire.* September 9. Accessed August 13, 2025. https://www.doctorgreenhouse.com/blog/vpd-the-pressure-to-transpire.

Stober, Willy, and Hillary Weitze. 2024. *Controlled Environment Horticulture: Energy Consumption and Environmental Control Field Study.* Final Project Report, Pacific Gas and Electric Company.

UC Davis College of Agricultural and Environmental Sciences. 2025. *Controlled Environment Agriculture.* September 4. Accessed April 6, 2026. https://caes.ucdavis.edu/research/initiative/controlled-environment-agriculture.

Appendix

Total Capacity	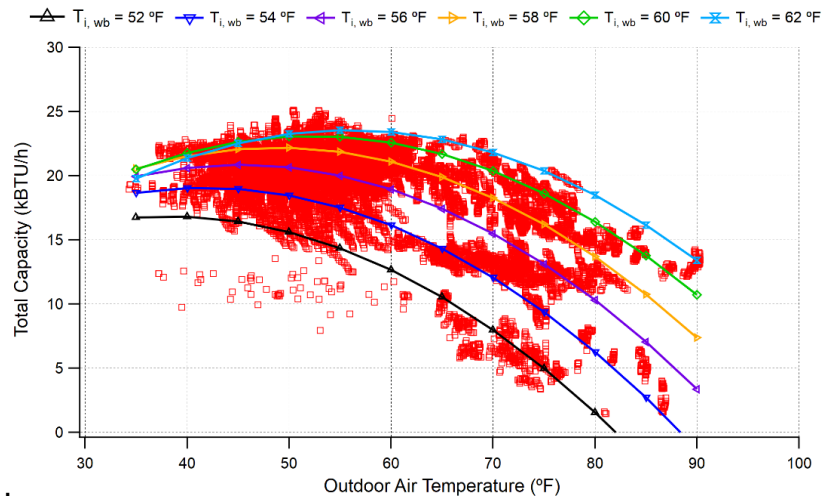
SHR	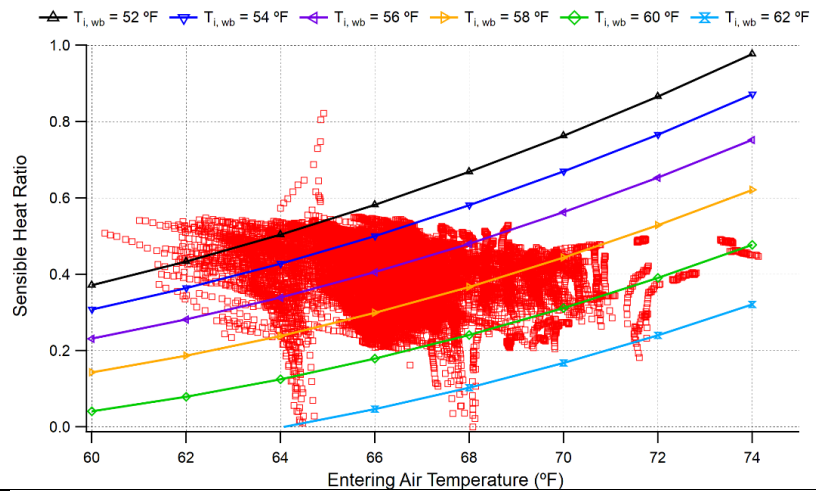
Power Draw	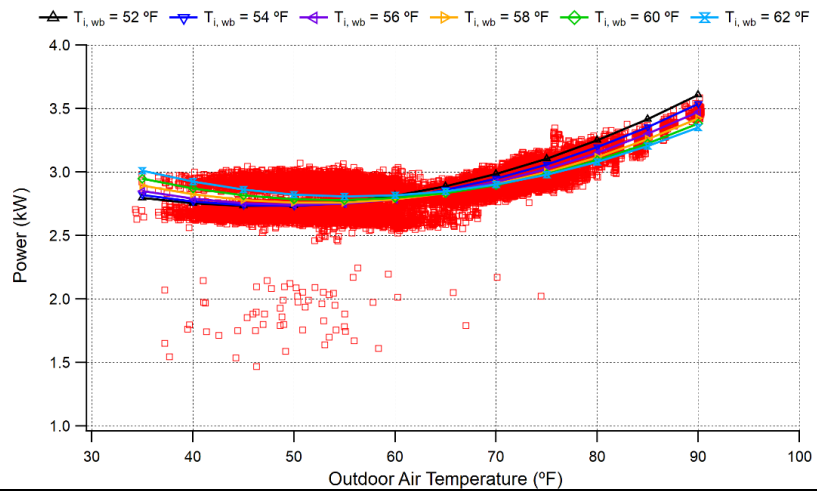

Figure 24: Modeled performance curves for the retrofit system, cool mode.

Total Capacity	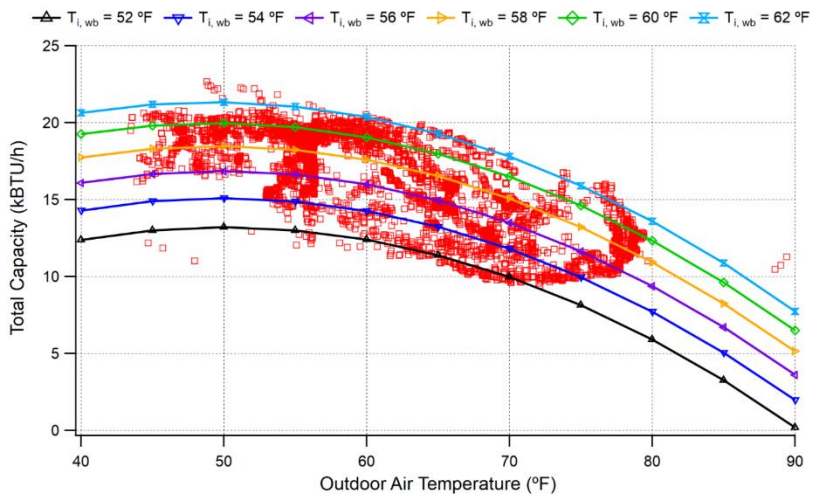
SHR	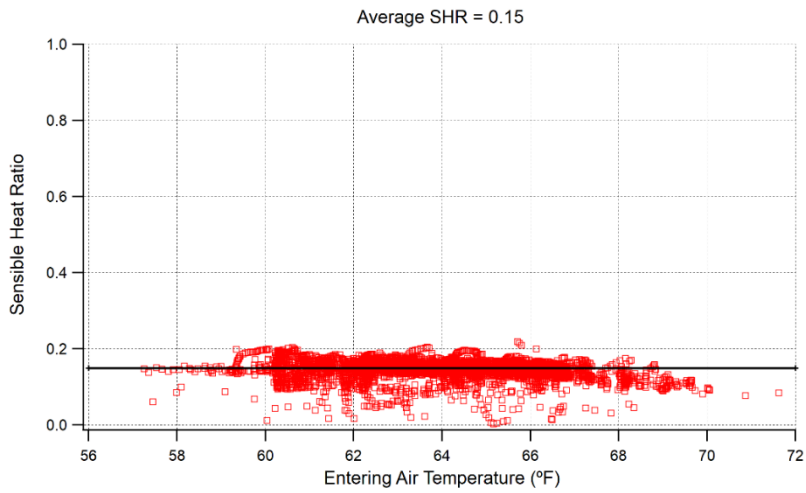
Power Draw	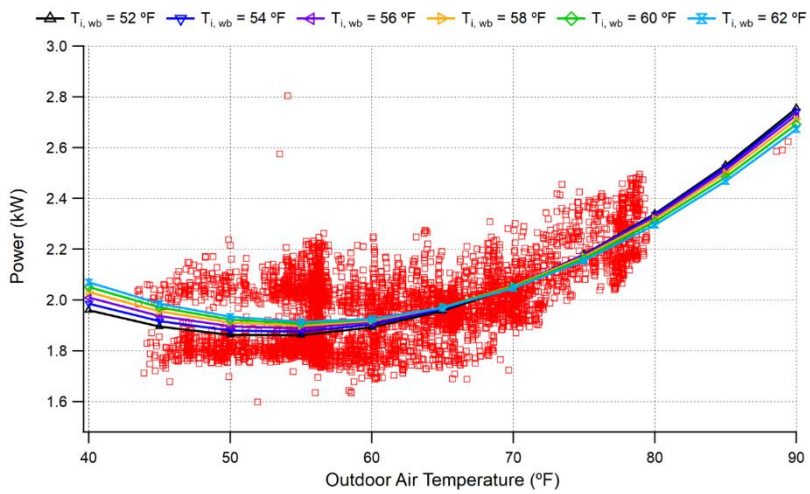

Figure 25: Modeled performance curves for the retrofit system, dehumidify mode.

Total Capacity	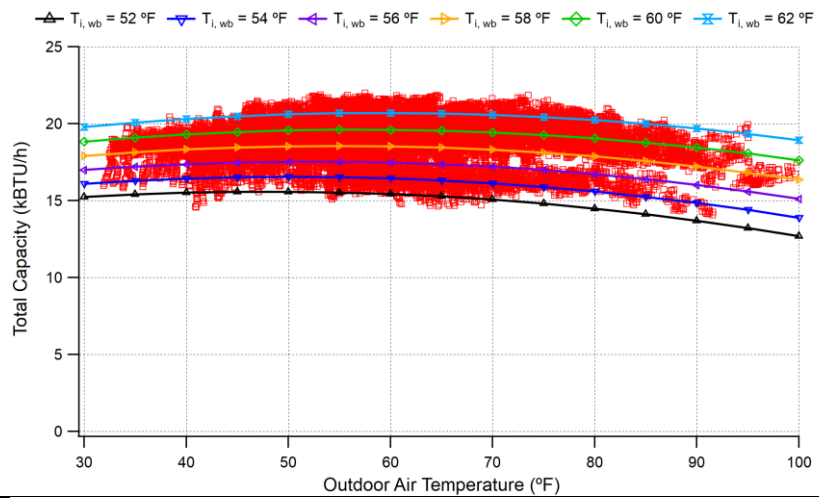
SHR	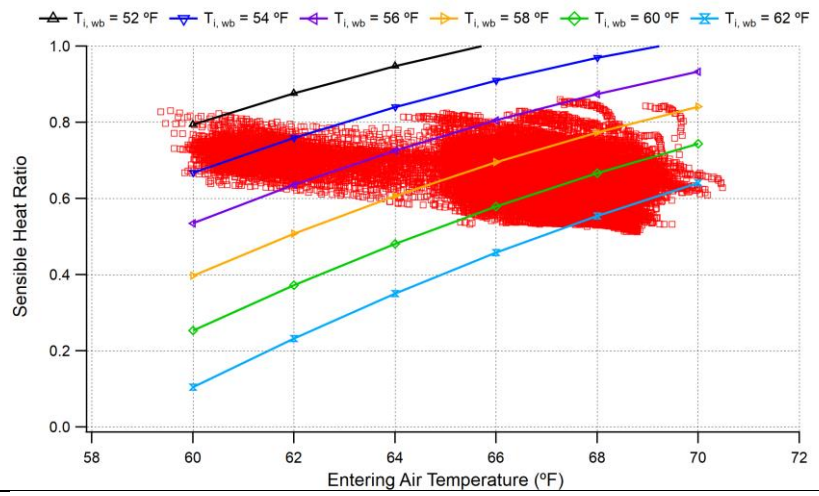
Power Draw	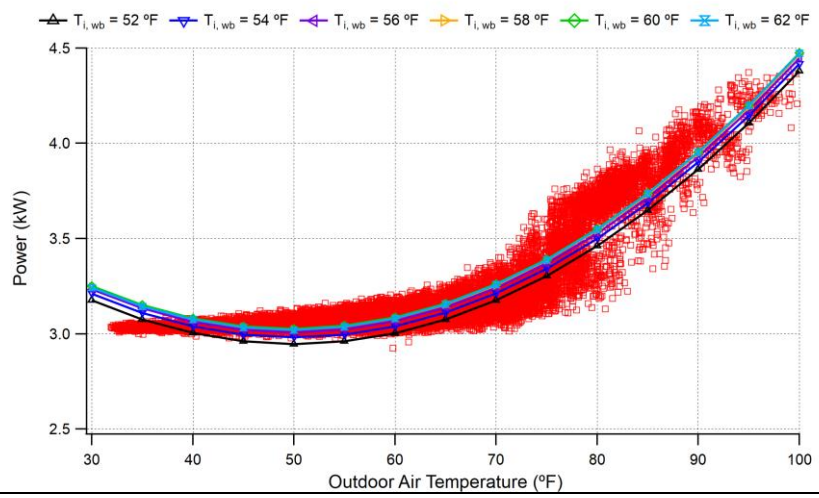

Figure 26: Modeled performance curves for baseline HVAC, cool mode.